MECHANISMS OF SYNERGISTIC ANTITUMOR EFFECT OF NAPROXEN AND SORAFENIB IN HEPATOCELLULAR CARCINOMA

A THESIS SUBMITTED TO
THE GRADUATE SCHOOL OF NATURAL AND APPLIED SCIENCES
OF
MIDDLE EAST TECHNICAL UNIVERSITY

BY

ETKİN AKAR

IN PARTIAL FULFILLMENT OF THE REQUIREMENTS
FOR
THE DEGREE OF MASTER OF SCIENCE
IN
BIOLOGY

JANUARY 2023

Approval of the thesis:

MECHANISMS OF SYNERGISTIC ANTITUMOR EFFECT OF NAPROXEN AND SORAFENIB IN HEPATOCELLULAR CARCINOMA

submitted by **ETKİN AKAR** in partial fulfillment of the requirements for the degree of **Master of Science** i**n Biology, Middle East Technical University** by,

Prof. Dr. Halil Kalıpçılar
Dean, Graduate School of **Natural and Applied Sciences** _____

Prof. Dr. Ayşe Gül Gözen
Head of the Department, **Biology** _____

Prof. Dr. Mesut Muyan
Supervisor, Biology**, METU** _____

Dr. Deniz Cansen Kahraman
Co-Supervisor, Health Informatics**, METU** _____

Examining Committee Members:

Assoc. Prof. Dr. Salih Özçubukçu
Chemistry, METU _____

Prof. Dr. Mesut Muyan
Biology, METU _____

Assist. Prof. Dr. Dilek Çevik
Medical School, Yüksek İhtisas University _____

Date: 23.01.2023

I hereby declare that all information in this document has been obtained and presented in accordance with academic rules and ethical conduct. I also declare that, as required by these rules and conduct, I have fully cited and referenced all material and results that are not original to this work.

Name Last name: Etkin Akar

Signature:

ABSTRACT

MECHANISMS OF SYNERGISTIC ANTITUMOR EFFECT OF NAPROXEN AND SORAFENIB IN HEPATOCELLULAR CARCINOMA

Akar, Etkin
Master of Science, Biology
Supervisor: Prof. Dr. Mesut Muyan
Co-Supervisor: Dr. Deniz Cansen Kahraman

January 2023, 86 pages

Hepatocellular carcinoma (HCC) is life-threatening cancer that accounts for the second leading cause of cancer-related deaths worldwide. Due to the complexity and heterogeneity of HCC, which leads to resistance to current targeted therapies, combination therapy becomes an important strategy. Since 90% of HCC arises from chronic liver inflammation, HCC drugs combined with non-steroid anti-inflammatory drugs (NSAIDs) are considered an important strategy to increase treatment efficacy. In this study, we aimed to find a synergistic interaction between FDA-approved NSAIDs and HCC drugs and investigate the mechanism behind their synergistic interaction. Among all combinations, Naproxen and Sorafenib were found to be synergistically interacting in HCC. Network reconstruction analysis was performed to investigate the mechanism implicated in this drug combination. Apoptosis pathways were enriched in both Sorafenib and Naproxen networks which were further supported by Annexin V/PI staining, Hoechst staining, and analysis of apoptosis-related proteins in HCC cell lines. Our results pointed out that apoptosis induction could be associated with the down-regulation of the CAPN2 gene and decreasing the activity of PI3K/AKT pathway in HCC.

Keywords: Synergy, NSAIDs, HCC, Sorafenib, Naproxen, apoptosis

ÖZ

HEPATOSELÜLER KARSINOMDA NAPROXEN VE SORAFENIB SINERJISTIK ETKILEŞIM MEKANIZMASININ AYDINLATILMASI

Akar, Etkin
Yüksek Lisans, Biyoloji
Tez Yöneticisi: Prof. Dr. Mesut Muyan
Ortak Tez Yöneticisi: Dr. Deniz Cansen Kahraman

Ocak 2023, 86 sayfa

Hepatoselüler karsinoma (HSK) dünya üzerinde ölüme sebebiyet veren başlıca kanser türlerinden biridir. HSK'nın heterojen yapısı güncel tek hedefli yaklaşımlarda sınırlı sağ kalım saglamakta ve birden çok mekanizmanın hedef alındığı kombine terapiler kanser tedavisinde önemli bir strateji olarak görülmektedir. HSK; inflamasyon bağlantılı bir kanser olduğu ve birçok çalışmada non-streoid anti-inflamatuvar ilaçların (NSAİİ) anti-kanser aktivitesi gösterildiği için, NSAİİ ve HSK ilaçlarının kombine edilmesi önemli bir strateji olarak düşünülmektedir. Bu çalışmadaki amaç; HSK 'da kullanılan güncel ilaçlarla, NSAİİ'ler arasında sinerjistik etki bulmak ve bu etkinin HSK üzerindeki mekanizmasının aydınlatılmasıdır. Bu çalışmada Naproxen ve Sorafenib ilaç kombinasyonunun HSK üzerindeki sinerjistik etkisi gösterilmiş olup, hücresel sinyal yolaklarının yeniden yapılandırma analizi ile, apoptoz yolaklarının her iki ilaçta aktitivesinin arttığı gösterilmiş ve deneysel yöntemlerle; Annexin V/PI boyaması, Hoecst boyaması ve western blot analizleri ile doğrulanmıştır. Ayrıca, apoptoz indüklenmesinin PI3K/AKT sinyal yolağı aktivitesi ve CAPN2 ifadesindeki azalmayla bağlantılı olabileceğine işaret edilmiştir.

Anahtar Kelimeler: Sinerji, NSAİİ, HSK, Sorafenib, Naproxen, Apoptoz

To my precious family,

ACKNOWLEDGMENTS

Firstly, I would like to express my deepest gratitude to my precious supervisor Dr. Deniz Cansen Kahraman, for her guidance, support, encouragement, and trust. She is a great mentor, that I could not have undertaken this journey without her. She was always there when I struggled means a lot to me.

I am deeply indebted to my advisor Prof. Dr. Mesut Muyan, for his constructive criticism of this study and sharing his knowledge with us. Moreover, I always appreciate him for accepting me as an inexperienced undergraduate student in his lab; this enlightened me to realize what I want in my career path.

I would like to thank Assoc. Prof. Dr. Salih Özçubukçu and Assist. Prof. Dr. Dilek Çevik, for accepting to be a member of my thesis committee.

I am grateful to Assoc. Prof. Tunca Doğan for his tangible support during my master's. I am also thankful to Prof. Dr. Rengül Çetin Atalay for allowing being a member of CanSyL and for her support of my career in science.

I would like to extend my thanks to my past and present CanSyL members Altay Koyaş, Esra Nalbat, Tuğçe Gül Karahan, Ece Kalem, and Büşra Bınarcı for their emotional support and friendship during my master journey. I'd like to express my gratitude to my precious family, my deceased father Adil, my mother Fitnat, and my brother Onur for their belief in me. Finally, I am thankful to my friends; Volkan, Ceren, Sinem, Rana, Seçkin, and Alper for their friendship.

This study was supported by the Ministry of Development, CanSyL Project (Grant id: 2016K121540).

TABLE OF CONTENTS

ABSTRACT v

ÖZ vi

ACKNOWLEDGMENTS viii

LIST OF TABLES xiii

LIST OF FIGURES xiv

LIST OF ABBREVIATION xvi

CHAPTERS

1 INTRODUCTION 1

1.1 Hepatocellular Carcinoma 1

1.1.1 Risk Factors for HCC 1

1.1.2 Chronic Inflammation and HCC 2

1.2 Available HCC Treatment Options 3

1.2.1 Systemic Therapy 3

1.3 Combination Therapy in Hepatocellular Carcinoma 4

1.4 Concept of Drug Synergism 5

1.5 Non-steroid Anti-inflammatory Drugs (NSAIDs) 6

1.5.1 NSAIDs in Cancer 6

1.5.2 Naproxen in Cancer 7

1.6 Pathway Analysis in Cancer Research 7

1.7 Function of CAPN2 in Cancer 8

1.8 Apoptosis in Cancer 8

1.9 Important Pathways in HCC 10

1.9.1 Akt Pathway 10
2 MATERIALS AND METHOD 13
2.1 Materials 13
2.1.1 Cell Culture Materials 13
2.1.2 Cytotoxicity Assay Reagents 14
2.1.3 Apoptosis and Cell Cycle Analysis Reagents 15
2.1.4 Western Blot Reagents 16
2.1.5 RNA isolation, cDNA synthesis and polymerase chain reaction (PCR) reagents and Instruments 18
2.1.6 Oligonucleotides 19
2.1.7 General Reagents 20
2.2 Solutions and Media 21
2.2.1 Cell Culture solutions 21
2.2.2 NCI-SRB assay solutions 21
2.2.3 PI staining solutions 22
2.2.4 Western blot solutions 22
2.3 Method 23
2.3.1 Cell Culture Methods 23
2.3.2 Synergyfinder Tool 26
2.3.3 Real-Time Cell Analyzer System 26
2.3.4 Pathway Analysis 27
2.3.5 Annexin-V/PI staining 28
2.3.6 Immunohistochemistry staining with Hoechst 33258 fluorescent dye …….. 29

2.3.7 Western Blot 30
2.3.8 Gene expression analysis 33
2.3.9 Cell Cycle analysis with PI staining 36
2.3.10 Statistical Analysis 36
3 RESULTS 39
3.1 Selection of synergistically interacting anti-inflammatory drugs and anti-cancer drug pairs in hepatocellular carcinoma cell lines 39
3.1.1 Effect of other combinations in HCC cell lines 42
3.1.2 Effect of combination in normal like fibroblast cells 42
3.1.3 Cytotoxic effect of the selected concentration of naproxen and sorafenib combination against HCC cell lines. 42
3.1.1 Observation of real-time cell proliferation curve of sorafenib and naproxen against HCC cell lines 43
3.1.2 The morphological changes of HCC cells upon drug combination 44
3.2 Network Analysis of Sorafenib and Naproxen 46
3.2.1 Determination of differentially expressed genes of Naproxen and Sorafenib treated cells 46
3.2.2 Network analysis of sorafenib and Naproxen in Huh7 cells 47
3.2.3 Gene enrichment analysis in Sorafenib and Naproxen Network 49
3.3 Sorafenib and Naproxen combination induce apoptosis in HCC cell lines. …. 50
3.4 Combination induces G1 arrest in HCC cell lines 58
3.5 Investigation of CAPN2 gene in Hepatocellular Carcinoma 58
3.6 Investigation of PI3K pathway activity upon drug combination in HCC cell line 61

4 CONCLUSION AND DISCUSSION 65

5 FUTURE PERSPECTIVES 69

REFERENCES 71

APPENDICES

A. SUPPLEMENTARY FIGURES 81

LIST OF TABLES

TABLES

Table 2.1.1: Cell Culture reagents and equipment 13
Table 2.1.2: Reagents for NCI-SRB Assay and RT-CES experiments 14
Table 2.1.3: Reagents for apoptosis and cell cycle analysis 15
Table 2.1.4: Reagents for Western Blot 16
Table 2.1.5: Primary antibodies used in western blot 17
Table 2.1.6: Secondary antibodies used in western blot 18
Table 2.1.7: Reagents and equipment used in RNA isolation, cDNA synthesis and PCR 18
Table 2.1.8: Primers used in this study 19
Table 2.1.9: General reagents used in the experiments 20
Table 2.3.1: Number of cells seeded in 96-well plate 24
Table 2.3.2: Number of cells seeded for each incubation time in six-well plates .. 29
Table 2.3.3: Number of cells seeded in 10mm dishes for different time points 34

LIST OF FIGURES

FIGURES

Figure 1. 1 Risk Factors for HCC onset 2
Figure 1. 2 Schematic overview of apoptosis signaling. Extrinsic and intrinsic apoptosis pathways are represented. 10
Figure 2.3 1: Template for SRB Assay. 25
Figure 2.3 2: Pipeline for network reconstruction 28
Figure 3. 1 Naproxen and Sorafenib show synergistic interaction in HCC cell lines. 41
Figure 3.1. 1 The Selected synergistic concentration of Sorafenib and Naproxen combination decreases cell viability against HCC cell lines. 43
Figure 3.1. 2 Real time cell growth analysis of HCC cells treated with selected concentrations of the drugs. 44
Figure 3.1. 3 Morphological changes of Mahlavu and Huh7 cells in different time points 45
Figure 3.2 1 Venn diagram representation of differentially expressed genes in sorafenib and naproxen treated cell. 47
Figure 3.2 2 Network analysis of Sorafenib and Naproxen in HCC cell line. 48
Figure 3.2 3 Representation of pathway enrichment result of Sorafenib and Naproxen in HCC cell line. 49
Figure 3.3. 1 Hoechst staining of HCC cells in 24h, 48h, 72h of treatment. 53
Figure 3.3. 2 Flow cytometry analysis of Annexin-V/PI staining and bar graph representation of late apoptotic cells. 55
Figure 3.3. 3 Western blot analysis of apoptosis signaling proteins in HCC cell lines 57
Figure 3.5. 1 CAPN2 expression is upregulated in HCC cell upon treatment with Sorafenib, Regorafenib, and Lenvatinib. 59
Figure 3.5. 2 Upregulation of CAPN2 associated with low rate of overall survival of patients 59

Figure 3.5. 3 CAPN2 relative mRNA expression in HCC cell lines. 60
Figure 3.6. 1 Drug combination decreases activity of PI3K-AKT pathway..... 63
Figure A.1 Effect of other combination in HCC cell lines. 83
Figure A.2 Effect of combination on MCF12A -normal like cell line. 84
Figure A.3 Annexin-V assay of sorafenib and naproxen combination..... 85
Figure A.4 Cell cycle analysis of sorafenib and naproxen combination in HCC cell lines. 86

LIST OF ABBREVIATION

AKT	Serine/Threonine protein kinase
BCA	Biocinchoninic acid assay
BCL-2	B cell Lymphoma gene 2
BSA	Bovine serum albumin
CAPN2	Calcium activated neutral proteinase
CASPASE	Cysteine aspartic acid protease
cDNA	Complementary DNA
CI	Cell index
Cq	Quantitative cycle
qRT-PCR	Quantitative Reverse Transcription PCR
ddH_2O	Double-distilled water
dH_2O	Distilled water
dNTP	Deoxyribonucleoside triphosphate
DMEM	Dulbecco's Modified Eagle's medium
DMSO	Dimetyl Sulfoxide
DNA	Deoxyribonucleic acid
DTT	Dithiothreitol
EtOH	Ethanol
FBS	Fetal bovine serum
FDA	Food and drug administration
FOXO	Forkhead box O
HBV	Hepatitis B Virus
HCC	Hepatocellular Carcinoma
HCV	Hepatitis C Virus
IC	Inhibitory concentration
mRNA	Messenger RNA

Mtor	Mammalian target of rapamycin
NP-40	Nonidet P-40
OD	Optical density
PARP	Poly ADP-ribose polymerase
PBS	Phosphate-buffered saline
PI	Propidium iodide
RNA	Ribonucleic acid
RT	Room temperature
RTCEs	Real-time cell electronic sensing
SDS	Sodium dodecyl sulfate
SRB	Sulforhodamine B assay
TBS	Tris buffered saline
TBS	Tris-base
TBS-T	Tris buffered saline with Tween 20
TCA	Trichloroacetic acid

CHAPTER 1

INTRODUCTION

1.1 Hepatocellular Carcinoma

Liver cancer is among the most challenging cancers, as over 1 million people are expected to be diagnosed by 2025. Approximately 850.000 people are diagnosed with liver cancer every year. Hepatocellular carcinoma (HCC) is considered the most common type of liver cancer, which accounts for %90 of all cases and second leading cause of cancer-related deaths worldwide. (Llovet et al., 2021)

1.1.1 Risk Factors for HCC

HCC is a complicated and heterogenous malignancy exacerbated by many risk factors. Some factors are well known for considering the developing risks for HCC, which include HBV (Hepatitis B virus) and HCV (Hepatitis C virus) infections, excessive alcohol consumption, non-alcoholic fatty liver disease, and ingestion of some toxins such as aristolochic acid and aflatoxins. Figure 1.1. shows cooperating risk factor HCC onset (Refolo et al., 2020). It is important to highlight the risk factors of HCC since they are mostly preventable and may reduce the burden of HCC worldwide (J. D. Yang et al., 2019).

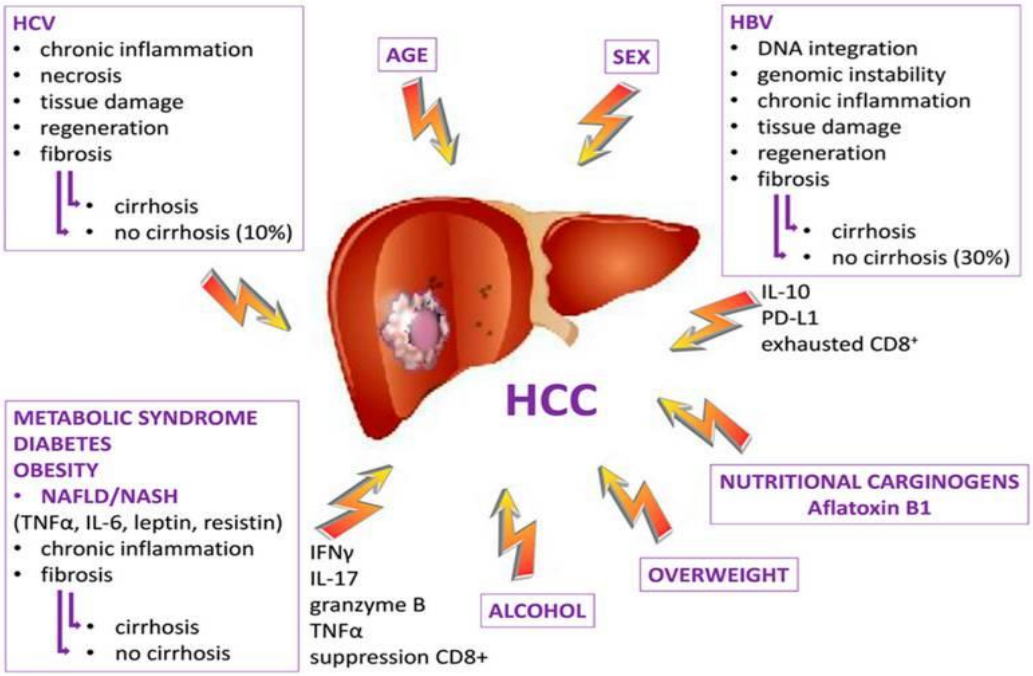

Figure 1. 1 Risk Factors for HCC onset.

1.1.2 Chronic Inflammation and HCC

Inflammation is a strictly regulated body defense mechanism to remove harmful stimuli and pathogens from the body. It is an adaptive response against tissue infection and injury. It is characterized by increasing blood vessels to the site of infection, followed by immune cell recruitment and subsequent release of inflammatory mediators. Although inflammation is a well-controlled process, sometimes it gets out of control because of the persistent danger stimulus and infection or uncontrolled regulatory mechanism, eventually resulting in chronic inflammation (Yu et al., 2018). Chronic inflammation is related to the risk of developing many cancer types, including HCC, colon and breast cancer. Among these, one of the most studied cancer types associated with inflammation is HCC. Approximately 90% of HCC cases arise from chronic liver inflammation. The risk factors, such as HBV, HCV, diabetes, etc., are considered to promote chronic inflammation and are associated with the onset of HCC (Refolo et al., 2020). In viral

hepatitis infection, host immune cells often cannot eradicate the infection, which makes antigen-specific immune response persist (Budhu & Wang, 2006). These host-immune cells activated to kill virus-infected cells starts producing several cytokine and growth factors to compensate for the burden of infection(Markiewski et al., 2006). This continued cycle of necro inflammation and hepatocyte regeneration deregulates the proliferation pathway (Hayato & Shin, 2012) eventually contributing to the development of HCC.

Besides these etiological factors, such as HBV and HCV infections, another denominator factor for HCC progression is parenchymal cell death, resulting in a persistent wound-healing response that ultimately activates an inflammatory cascade. Overall, continuous inflammation leads to chronic liver injury, transforming into dysplasia and eventually HCC (Bishayee., 2014).

1.2 Available HCC Treatment Options

Treatment options are considered to the patient's diagnosis stage and overall health. If HCC is diagnosed at early stages, liver resection, transplantation, and ablation could potentially be therapeutic (J. D. Yang et al., 2019). If the surgical resection is inconvenient, radiofrequency and microwave ablation can be considered therapeutic options. However, unfortunately, most HCC cases are diagnosed at late stages, and systemic chemotherapeutic drugs remain the only option. (Yang et al., 2019).

1.2.1 Systemic Therapy

Most hepatocellular carcinoma patients are diagnosed in very late stages, so systemic therapy remains the only option. For more than a decade, Sorafenib was the only chemotherapeutic drug approved by the Food and Administrative Department (FDA) for the treatment of advanced HCC between 2007 and 2016. During these years, all first and second-line studies were unsuccessful and could not be approved by the FDA. However, with the improvement in knowledge of molecular cell biology,

understanding the mechanism of disease and its progression led to the discovery of new small molecules that target specific pathways and proteins, providing new opportunities for molecular-targeted therapy. Lenvatinib, Regorafenib, Cabozantinib, and Ramucirumab, were approved by the FDA for HCC between 2017 and 2019(H. Zhang et al., 2022). Although approved drugs share some similar targets, they differ in their mechanism of action. Sorafenib is a multikinase inhibitor that targets RAS/MEK/ERK signaling; inhibits vascular endothelial growth factor receptor (VEGFR) and platelet-derived factor (PDGFR). Therefore, it targets proliferation and angiogenesis pathways implicated in the pathogenesis of HCC (Zhang et al., 2022). Lenvatinib is also the first line treatment as Sorafenib. It is an inhibitor of fibroblast growth factor receptor (FGFR), PDGFR, KIT, and RET. It differs from Sorafenib by targeting Fibroblast growth factor (FGF) pathways. On the other hand, Regorafenib is the first small molecule inhibitor approved as second-line therapy for HCC. It is safe for patients who develop sorafenib resistance (Sanduzzi-Zamparelli et al., 2019). Although the mechanism of action is similar to Sorafenib, Regorafenib also targets oncogenic mutants of KIT, RET, and BRAF, which show increased levels in HCC (Tai et al., 2014) The main targets for Cabozantinib are c-MET, VEGFR, and AXL protein (Deng et al., 2021). On the other hand, Ramucirumab is a human G1 monoclonal antibody against VEGFR-2. It is a competitor of VEGF and blocks downstream pathways of VEGF signaling (Roviello et al., 2019). Although identifying new drugs for advanced HCC patients allows some improvement, the survival rate still ranges from 6 to 12 months for patients with advanced HCC (H. Zhang et al., 2022).

1.3 Combination Therapy in Hepatocellular Carcinoma

As discussed in section 1.2.4, only early diagnosis can be treated with surgical methods, but for the advanced HCC, chemotherapeutic drugs are considered as a treatment strategy. Despite the treatment options and systemic therapeutics drugs, patients with advanced HCC have relatively poor long-term prognosis (J. Yang et

al., 2012). Due to the complexity and heterogeneity of HCC, targeted treatment with FDA-approved drugs show a limited survival advantage. It has been demonstrated that only ~30% of patients are responsive to sorafenib treatment and the median of overall survival was approximately 2.8 months increased (Llovet et al., 2008). Therefore, there needs to be an urgent effort to improve the efficacy of the current treatment options. One study stated that multi-targeted treatments have therapeutic benefits by enhancing the treatment efficacy and avoiding the acquisition of monotherapy resistance (Wood et al.,2014). Many studies show that cancer drugs eventually result in resistance and dramatic side effects when they are used in the long term (Lippert et al., 2008), (Kelderman et al., 2014). Therefore, to eliminate the resistance, possible side effects, and the possibility of reoccurrence, combinatorial drug treatment approaches have been extensively studied (Mokhtari et al., 2017) (Wang et al., 2019) (Jia et al., 2009).Moreover, in the line of HCC, many studies showed that combining Sorafenib with different small molecule inhibitors increases the anti-tumor activity of Sorafenib and has a better outcome on other HCC cell lines compared to administration of Sorafenib alone (Yao et al., 2020), (Hsu et al., 2017),(Yao et al., 2020). It has been shown that combination of Sorafenib with anti PD-1 show better survival benefit and treatment efficacy compared to anti-PD-1 treatment alone (Chen et al., 2022). One other study showed that combining a low dose of Sorafenib with celecoxib (non-steroid anti-inflammatory drug) synergistically inhibits cell viability via Akt and RAS/RAF pathways (Morisaki et al., 2013). Another study also reveals the mechanism behind the synergistic interaction of Sorafenib and Aspirin in HCC (Xia et al., 2017). Therefore, based on the evidence from many studies, combination treatment represents a significant direction for the systemic treatments of HCC (Zhang et al., 2022).

1.4 Concept of Drug Synergism

Synergy is described as an effect of each drug that is intensified when used concurrently. In other words, the combinatory effect is greater than the sum of the

individual effect of each drug (Roell et al., 2017). Drug synergism is an important concept since it reduces drug dose and side effects; it could also interfere with undesired resistance mechanisms (Duarte & Vale, 2022). As shown in many studies, sorafenib is administrated with a low dose (2.5μM-5μM), when it is combined with other small molecules that have synergistic interaction (Omar et al., 2016), (Morisaki et al., 2013). Moreover, some other studies show that the synergistic interaction of sorafenib with small molecule inhibitors targets resistance mechanisms (Rausch et al., 2010)(Lei et al., 2019).

1.5 Non-steroid Anti-inflammatory Drugs (NSAIDs)

1.5.1 NSAIDs in Cancer

Non-steroidal anti-inflammatory drugs have been used to reduce pain and inflammation for many years (Wehling, 2014). Since a close association between inflammation and HCC development has been described, non-steroidal anti-inflammatory drugs have been under investigation for a long time. Based on many clinical and experimental studies, variable NSAIDs could reduce the incidence and progression of some cancer types, including gastric, breast, HCC, and colon (Pang et al., 2017). A study conducted by the National Institutes of Health-AARP Diet among 300504 men and women showed that there had been a link between aspirin usage and the risk of HCC incidence. Aspirin usage significantly reduced the risk of HCC incidence compared to the group that did not use aspirin(Sahasrabuddhe et al., 2012). Apart from cohort studies, several experimental studies show the anti-cancer activity of NSAIDs *in vivo* and *in vitro*. One study reveals that ibuprofen mediates its anti-tumor activity by targeting both the Wnt/β-catenin and NF-κB pathways (Rayburn et al., 2009). One other study shows that novel triazolothiadiazines NSAIDs, exert an anti-cancer effect in HCC via AKT and ASK-1 proteins (Aytaç et al., 2016). Therefore, numerous studies prove variable NSAIDs have anti-cancer

properties in different cancer types (Kahraman et al., 2022) (Greenspan et al., 2011)(Aytaç et al., 2016).

1.5.2 Naproxen in Cancer

Naproxen is a type of NSAID used in treatment of pain, acute gouty arthritis, migraine and inflammatory diseases such as rheumatoid arthritis. It was approved by FDA in 1976. Naproxen acts as a competitive inhibitor of arachidonate. It binds both COX-1 and COX-2, resulting in decreased levels of prostaglandin G(PGG) (Brutzkus, n.d.). Couple of studies showed that elevated levels of naproxen show anti-tumor effect (Motawi et al., 2014).Moreover, It is also shown that higher doses of Naproxen (0.5 to 2 mmol/L) induce G1 arrest and apoptosis in urinary bladder cancer cell lines by targeting PI3K (Kim et al., 2014).

1.6 Pathway Analysis in Cancer Research

Multiple pathways can be altered in cancer cells, and drugs not only perturb their immediate target but also modulate various signaling pathways in cells (Unsal-Beyge & Tuncbag, 2022). Considering the complex interactions between molecules or interactions within the cell, modulation of the drug target is not local. Therefore, exploring drug networks can reveal hidden proteins in cell signaling pathways (Unsal-Beyge & Tuncbag, 2022). Many studies show that network-based approaches may reveal many unknown drug responses in different cancer cell types (Guney et al., 2016) (Cheng et al., 2018) (Menche et al., 2015). Therefore, the drug network can be reconstructed to show the hidden target of the drugs besides their immediate target and signaling pathways modulated within this interaction (Unsal-Beyge & Tuncbag, 2022).

1.7 Function of CAPN2 in Cancer

CAPN2 is a member of the calcium-activated proteases family that can cleave various proteins in the cell, especially those that have a role in cytoskeletal remodeling and signaling. Growing body of research shows that CAPN2 is an important target for a variety of cancer types. CAPN2 upregulation promotes metastasis in different cancer types, including pancreatic and renal cell carcinoma. (Miao et al., 2017). (Peng et al., 2022). Also, CAPN2 upregulation was determined as a necessity for the progression of HCC. (Ma et al., 2022). Moreover, it has also been shown that its silencing promotes apoptosis in lung cancer (Zhang et al., 2018). Therefore, targeting CAPN2 could be a promising therapeutic option for cancer.

1.8 Apoptosis in Cancer

Apoptosis is a tightly regulated programmed cell death mechanism regulated by several signaling pathways in cells (extrinsic and intrinsic pathways). Apoptosis can occur when the cell undergoes stress, DNA damage, or immune surveillance (Carneiro & El-Deiry, 2020). It serves to remove any unwanted or unnecessary cells (Pfeffer & Singh, 2018).Apoptosis is characterized by DNA fragmentation in the nucleus, condensation of chromatin material, cell shrinkage, and loss of adhesion. Moreover, flip-flopping of phosphatidylserine and caspase activation are indicators of cell death (Elmore, 2007). Apoptosis can be divided into two cores of signaling; intrinsic and extrinsic apoptosis. The intrinsic apoptosis pathway, as the name implies, starts within the cell and does not require external stimulus (Wong, 2011)and is characterized by mitochondrial membrane permeabilization (MOMP) followed by cytochrome-c release to the cytoplasm. This leads to apoptosome assembly, which consists of cytochrome c, Apaf-1 and caspase-9 (Kroemer et al., 2007) and also leads to caspase-3 activation. (Carneiro et al,.2020). The release of cytochrome-c is closely mediated by the BCL-2 protein family that has both pro-apoptotic and apoptotic members. Bax, Bak, Bad, Bcl-Xs, Bid, Bik, Bim and Hr are

identified as pro-apoptotic members by stimulating cytochrome c release to the cytoplasm, whereas Bcl-2, Bcl-XL, Bfl-1, and Mcl-1 are identified as anti-apoptotic members by inhibiting cytochrome c release (Reed et al., n.d.). The balance between these two sub-groups regulates the intrinsic apoptotic pathway and determines whether apoptosis is initiated (Reed et al., n.d.). There are other apoptotic factors released from mitochondria to the cytoplasm, mainly including apoptosis-inducing factor (AIF), second mitochondria-derived activator of caspase (Smac). Smac serves as a promoter for caspase activation by binding to an inhibitor of apoptosis proteins (IAPs) (LaCasse et al., 2008). Eventually, this mechanism results in cell death. On the other hand, the extrinsic apoptosis pathway is initiated with an external stimulus. When death ligands such as TNF and FAS bind to the death receptor (e.g., TRAIL, TNFR1), conformation change occurs, and it subsequently recruits many adaptor proteins as well as caspase-8. This complex involves ligand, receptor, and adaptor proteins called Death-inducing Signaling Complex (DISC). Once DISC is assembled, caspase-8 is activated, which leads to subsequent activation of caspase-3 and triggers apoptosis (Wong., 2011). Extrinsic and intrinsic apoptosis pathway mechanisms are illustrated in Figure 1.2.2 (Jan et al., 2019).

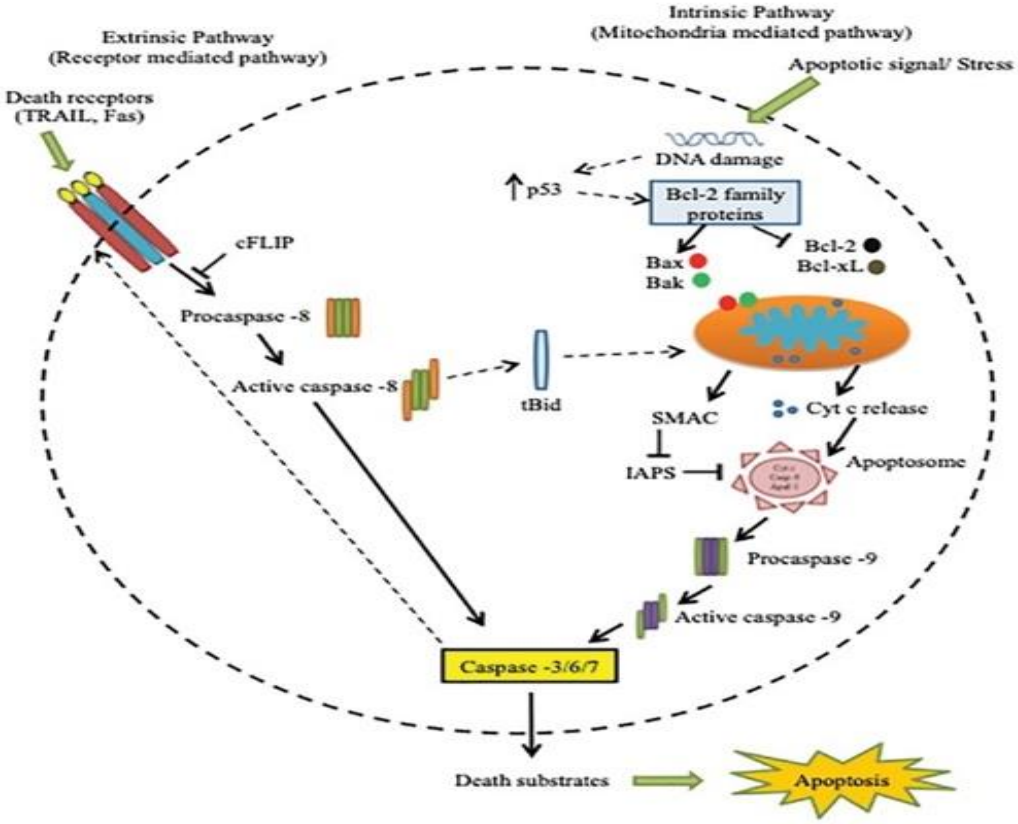

.

Figure 1. 2 Schematic overview of apoptosis signaling. Extrinsic and intrinsic apoptosis pathways are represented.

1.9 Important Pathways in HCC

1.9.1 Akt Pathway

As discussed in section 1.1.1, exposure to some virus, toxin, chemical, or other environmental factors leads to chronic liver injury and results in extensive cell death. It is consequently followed by hepatocyte regeneration due to continuous liver inflammation. This death and regeneration cycle triggers the activation of many signaling pathways, including the PI3K/AKT pathway. (Ozturk et al., 2006) (Llovet et al., 2008). Akt pathway dysregulation is involved in many cancer types (Buontempo et al., 2011). The serine/threonine kinase Akt is a well-known

downstream target of PI3K, which is located in the cytoplasm as an inactive state. The binding of Phosphatidylinositol (3,4,5)-trisphosphate to PI3K (PH) domain recruits AKT to the plasma membrane and enables its phosphorylation and subsequent activation (Hanada et al., 2004). Once AKT is activated, several downstream targets are phosphorylated, including FoxO transcription factors, Raf-1, BAD, and caspase-9, which are critical for cell survival. Moreover, PI3K/AKT pathway regulates BCL-2 family proteins by phosphorylating pro-apoptotic Bad, which is followed by the association of Bad with its adaptor proteins. This enables excess Bcl-2 or Bcl-X_L proteins to compete with Bax, thereby resulting in prevention of apoptosis (Chang et al., 2003). In the line of HCC, one study indicates that AKT activity is higher in the Mahlavu cell line in HCC compared to HepG2 and Huh7 (Buontempo et al., 2011). Overall, targeting the AKT pathway in hepatocellular carcinoma is considered an attractive therapeutic intervention in liver cancer.

CHAPTER 2

MATERIALS AND METHOD

2.1 Materials

2.1.1 Cell Culture Materials

All cell culture reagents, equipment including media, FBS, culture plates, cryovial, and the drugs that are used for this study are shown in Table 2.1.1

Table 2.1.1: Cell Culture reagents and equipment

Name	Manufacturer	Catalog no	Storage
Dulbecco's Modified Eagle's	Biological Industries	BI01-050- 1A	+4 °C
Phosphate-buffered saline	GibcoTM	14190	RT
Fetal bovine serum	GibcoTM	10270	-20 °C
Penicillin/streptomycin	GibcoTM	15140-122	-20 °C
Non-essential amino acids	Lonza	BE12-114E	+4 °C
L-glutamine	GibcoTM	25030	-20 °C
Trypsin-EDTA	GibcoTM	25200	-20 °C

Table 2.1.1 (cont'd)

Dimethyl Sulfoxide	Sigma-Aldrich	D2650	RT
Naproxen	Sigma-Aldrich	N8280-5G	RT
Sorafenib	Selleckchem	S7397	-20 °C
Ibuprofen	Sigma-Aldrich	F8514	RT
Flurbiprofen	Sigma-Aldrich	F8514-1G	RT
Aspirin	Sigma-Aldrich	N8280	RT
Doxorobicine	DABUR	7AA015	+4 °C
Serological pipettes, sealed-	Costar Corporation	NI	RT

2.1.2 Cytotoxicity Assay Reagents

The Regents required for SRB assay and real time RT-CES experiments are shown in table 2.1.2

Table 2.1.2: Reagents for NCI-SRB Assay and RT-CES experiments

Name	**Manufacturer**	**Catalog no**	**Storage**
Sulforhodamine B	Sigma-Aldrich	2S1403	RT
Trichloroacetic acid	Sigma-Aldrich	27242	+4 °C
Acetic acid	Sigma-Aldrich	27725	+4 °C

Table 2.1.2 (cont'd)

E-plates (96 well)	ACEA Biosciences	5232368001	RT

Microplate reader from BMG Labtech- SuperStar Nano instrument is utilized to get OD absorbance values in NCI-SRB; SRB Clonefill instrument from Genetix is used for washing steps.

A real-time cell analyzer platform was utilized as a place for E-plates (96-well); they were from Agilent Technologies.

2.1.3 Apoptosis and Cell Cycle Analysis Reagents

Parmingen-BD Annexin-V assay kit was utilized to perform apoptosis analysis via Novocyte flow cytometry instrument (ACEA Biosciences), whereas fixed cells stained with Hoechst 33258 fluorescent dye were observed under the fluorescent microscopy (Nikon elipse 5i with the ds-fi camera, Japan). PI staining was used to profile cell cycle phases via Novocyte flow cytometry instrument. The reagents that were used in the experiments are listed in Table 2.1.3

Table 2.1.3: Reagents for apoptosis and cell cycle analysis

Name	**Manufacturer**	**Catalog no**	**Storage**
FITC Annexin V Apoptosis Detection	Parmingen, BD	556547	+4 °C
Hoechst 33258 dye	Sigma-Aldrich	33258	+4 °C
Coverslips	Marienfeld	NI	RT
Propidium Iodide	Sigma Aldrich	P4864	+4 °C
Rnase A	Fermantes	EN0531	-20 °C

2.1.4 Western Blot Reagents

All the reagents that were used in western blot are shown in Table 2.1.4

Table 2.1.4: Reagents for Western Blot

Name	Manufacturer	Catalog no	Storage
Protease Inhibitor Cocktail Tablet	Roche	5892970001	+4 °C
PhosStop Tablet	Roche	4906837001	+4 °C
DTT	Carlo Erba	3086612	RT
Bicinchoninic Acid Protein Assay Kit	Sigma Aldrich	B9643	RT
Chameleon® Vue Pre-stained Protein Ladder	Li-cor	928-50000	-20°C
4X Protein Sample Loading Buffer	Li-cor	928-40004	RT
Mini PROTEAN TGX Stain-Free Gels	Bi-Rad	4568043-46	+4 °C
10X Tris/Glycine/SDS (TGS) Running Buffer	Bio-Rad	161-0772	RT
Western Blot Running Tanks, Transfer instrument, Power supply	Bio-Rad	NI	RT

Table 2.1.4 (cont'd)

Trans Blot Turbo 5X Transfer Buffer	Bio-Rad	10026938	+4 °C
Trans Blot LF PVDF Membrane and Filter Papers	BioRad	1620260	RT

The imaging instrument of the blot is Odyssey-CLx device (LICOR).

The primary and the secondary antibodies that were used in fluorescent system western blotting were listed Table 2.1.5 and Table 2.1.6, respectively.

Table 2.1.5: Primary antibodies used in western blot

Name	**Manufacturer**	**Catalog no**	**Dilutions**
PARP	CST	9532S	1:500
Caspase-9	Santa Cruz	Sc22182	1:100
Caspase-8	CST	9746S	1:100
Bcl-$x_{S/L}$	Santa Cruz	Sc634	1:100
Cytochrome-c	Santa Cruz	Sc7159	1:100
mTOR	CST	2983S	1:250
p-mTOR	CST	2971S	1:250
Akt	CST	9272S	1:500
P-Akt	CST	9271S	1:500
Calnexin	CST	2679S	1:2000
B-actin	CST	4967	1:2000

Table 2.1.6: Secondary antibodies used in western blot

Antibody Name	Manufacturer	Catalog No	Dilutions
680RD anti-rabbit	Li-cor	926-32211	1:10.000
680RD anti-mouse	Li-cor	926-32210	1:10.000
800CW anti Goat	Li-cor	925-32214	1:10.000

2.1.5 RNA isolation, cDNA synthesis and polymerase chain reaction (PCR) reagents and Instruments

RNA isolation, cDNA synthesis and DNAse treatments were done by using kits that shown in Table 2.1.7

Table 2.1.7: Reagents and equipment used in RNA isolation, cDNA synthesis and PCR

Name	Manufacturer	Catalog no	Storage
RNeasy Mini Kit	Qiagen	74106	RT
DNA-freeTM DNA Removal Kit	Invitrogen	AM1906	-20
RevertAid First Strand cDNA synthesis kit	Thermo Scientific	K1622	-20°C
10X Taq DNA Polymerase Buffer(+(NH4)2SO4,	Fermentas	NI	-20°C

Table 2.1.7 (cont'd)

Taq DNA Polymerase	Fermentas	NI	-20°C
Agarose	Sigma Aldrich	A9414	RT
2 mM dNTP	Fermentas	NI	-20°C
GeneRuler® 50 bp DNA ladder	BioLabs	N3236S	-20
Loading dye(6X)	Fermantas	R0611	+4 °C
Syber Green I Master Kit	Roche Applied Sciences	04 707 516 001	-20°C

Gel electrophoresis equipment and the power supply were from Cleaver Scientific. Gel images were taken in Bio-Rad Gel Doc EZ System.

Light Cycler® 96 Real-Time PCR system and Bio-Rad's T100 thermal cycler instrument are used to perform quantitative PCR and conventional PCR, respectively.

2.1.6 Oligonucleotides

All primers used in this study were synthesized in Oligomer Biotech and they were shown in the Table 2.1.8

Table 2.1.8: Primers used in this study

Genes	Primer Sequences	Amplicon size (bp)
AKT1	F: TCTATGGCGCTGAGATTGTG	113
	R: CTTAATGTGCCCGTCCTTGT	
GAPDH	F: TATGACAACGAATTTGGCTAC	115
	R: TCTCTCTTCCTCTTGTGCTCT	
CAPN2	F: TGCTCCATCGACATCACCAG	235
	R: GTCTGGTCAGCCTTTCCCTC	
RPL19	F: GCTCTTTCCTTTCGCTGCTG	155
	R: GGATCTGCTGACGCGAGTTG	
MTOR	F: CCAACAGTTCACCCTCAGGT	208
	R: GCTGCCACTCTCCAAGTTTC	

2.1.7 General Reagents

General reagents that were used in experiments are given as a Table 2.1.9.

Table 2.1.9: General reagents used in the experiments

Name	**Manufacturer**	**Catalog no**	**Storage**
Methanol	Carlo Erba	41272	RT
Ethanol	Sigma	E6133	RT
Acetic Acid	Sigma	27725	RT
Isopropanol	Sigma	34863	RT
Tween 20	Millipore	9005-64-5	RT
NaCl	Applichem	A4555-0250	RT

2.2 Solutions and Media

2.2.1 Cell Culture solutions

DMEM Complete Medium	10% Fetal Bovine Serum (FBS), 100 units/ml Penicillin/Streptomycin, 1% non-essential aminoacids, 2 mM L-Glutamine
Freezing Medium	10% DMSO in Fetal Bovine Serum (FBS)
DMEM- F12 growth medium	10% Fetal Bovine Serum (FBS), 2 mM L- Glutamine, 1% non-essential aminoacids, 20ng/ml EGF, 10 ug/ul insulin, %2,5 Hydrocortisone, 100-unit Penicillin/Streptomycin

2.2.2 NCI-SRB assay solutions

SRB stain solution	0.04 grams SRB dye dissolved in 10 ml 1% acetic acid solution.
10% TCA solution	100% TCA diluted to 10% in cold ddH_2O.

10 mM TrisBase	0.6 grams Tris dissolved in 500 ml cold ddH_2O.

2.2.3 PI staining solutions

50 ug/ml PI	1 mg/ml PI diluted to 50 ug/ml PI with 1xPBS
200ug/ml RNAse	10mg/ml RnaseA diluted to 200ug/ml RNAse with 1X PBS

2.2.4 Western blot solutions

NP-40 lysis buffer	150 mM NaCl, 50 mM TrisHCl (pH=8), 1% NP-40, 0,1% SDS, 1X protease inhibitor cocktail, 1X phosphoStop in ddH_2O
10X PhosStop	one tablet dissolved in 1 ml of ddH_2O
25X Protease Inhibitor Cocktail	one tablet dissolved in 1 ml of ddH_2O
10X Tris buffered saline (TBS)	12.2% (w/v) of Trisma base, 87.8% (w/v) of NaCl in 1 ml ddH_2O, pH=7.6

TBS-T	0.1% Tween-20 dissolved in 1X TBS
1X Tris/glycine/SDS (TGS) running buffer	10X TGS diluted to 1X TGS with cold dH_2O
Semi-dry transfer buffer (for 1 L)	200 ml 5X Trans-Blot Transfer Buffer, 600 ml cold ddH_2O, 200 ml EtOH
Mild stripping buffer (for 100 ml)	1.5 g Glycine, 1 ml Tween 20, 0.1 g SDS 100 ml ddH_2O, pH = 2.2

2.3 Method

2.3.1 Cell Culture Methods

In this study, Hepatocellular carcinoma cell lines Huh7 and Mahlavu cells were grown in complete DMEM, and Human Breast epithelial cells MCF12A were grown in DMEM/F12 media. All the cells were incubated at 37 °C in a 6% CO_2, incubator.

2.3.1.1 Thawing of frozen Cells

Frozen cells were taken from liquid nitrogen and immediately left in the water bath at 37°C for 1 minute. Then, cells were added to respective medium and centrifuged at 1500 rpm for 5 minutes. The supernatant was removed, and the cell pellet was resuspended with fresh medium and seeded on 10 mm dishes. The next day, depending on confluency, cells were either passaged or the medium was refreshed.

2.3.1.2 Sub-culturing and growth of cells

All the cells were regularly checked and once they reached %70-80 confluency, typically 3 days apart, cells were passaged by washing with 1X PBS and trypsinized for 3 minutes at 37 °C. Trypsin was added according to dish surface area; a 10 mm dish required 750 µL trypsin whereas; 6 well dishes required 350 µL trypsin. When cells were detached from the surface of the plate, they were collected into falcon tubes with fresh medium. Cells were thoroughly mixed by pipetting and directly transferred into 1.5 ml Eppendorf and counted by flow cytometry. Each cell line was seeded according to the required number of cells that were enough to grow in a particular dish area.

2.3.1.3 Cryopreservation of cells

Cells were trypsinized and collected into a 15 ml falcon. 80 µl cells were transferred to a 2 ml Eppendorf tube to be counted by flow cytometry, In the meantime, cells were centrifuged at 1500 rpm for 5 minutes, the supernatant was aspirated, the cell pellet was resuspended with freezing medium (10^6 cells /1 ml freezing medium/cryovial. Cells were transferred to cryovial and stored at -80°, then liquid nitrogen.

2.3.1.4 NCI-SRB Assay

Huh7, Mahlavu and MCF12-A cells were seeded into 96 well plates according to the optimized numbers that are indicated in Table 2.3.1.

Table 2.3.1: Number of cells seeded in 96-well plate

Cell line	**96 well plate (cell/well)**
Huh7	2500 cell/well

Table 2.3.1 (cont'd)

Mahlavu	1500 cell/well
MCF12A	5000 cell/ well

After 24h, the medium was removed and replaced with fresh 150 µl media. Dissolved drugs were applied to the respective well according to the plan that is shown in Figure 2.3.1 Sorafenib and Naproxen main stocks were prepared as 20 mM and 400 mM, respectively by dissolving with DMSO. For the treatment, according to the formula $M_{stock} * V_{stock} = M_{final} * V_{final}$; the required volume of each drug for each condition was calculated and applied to corresponding wells. The percentage of DMSO (used as a vehicle control) did not exceed 0.2% to avoid toxic effects on the cells.

DMSO	DMSO	DMSO	100 µM Naproxen	100 µM Naproxen	100 µM Naproxen	200 µM Naproxen	200 µM Naproxen	200 µM Naproxen	400 µM Naproxen	400 µM Naproxen	400 µM Naproxen
0.15 µM SOR	0.15 µM SOR	0.15 µM SOR	SOR 0.15 µM 100 µM Naproxen	SOR 0.15 µM 100 µM Naproxen	SOR 0.15 µM 100 µM Naproxen	SOR 0.15 µM 200 µM Naproxen	SOR 0.15 µM 200 µM Naproxen	SOR 0.15 µM 200 µM Naproxen	SOR 0.15 µM 400 µM Naproxen	SOR 0.15 µM 400 µM Naproxen	SOR 0.15 µM 400 µM Naproxen
0.3 µM SOR	0.3 µM SOR	0.3 µM SOR	SOR 0.3 µM 100 µM Naproxen	SOR 0.3 µM 100 µM Naproxen	SOR 0.3 µM 100 µM Naproxen	SOR 0.3 µM 200 µM Naproxen	SOR 0.3 µM 200 µM Naproxen	SOR 0.3 µM 200 µM Naproxen	SOR 0.3 µM 400 µM Naproxen	SOR 0.3 µM 400 µM Naproxen	SOR 0.3 µM 400 µM Naproxen
0.62 µM SOR	0.62 µM SOR	0.62 µM SOR	SOR 0.62 µM 100 µM Naproxen	SOR 0.62 µM 100 µM Naproxen	SOR 0.62 µM 100 µM Naproxen	SOR 0.62 µM 200 µM Naproxen	SOR 0.62 µM 200 µM Naproxen	SOR 0.62 µM 200 µM Naproxen	SOR 0.62 µM 400 µM Naproxen	SOR 0.62 µM 400 µM Naproxen	SOR 0.62 µM 400 µM Naproxen
1.25 µM SOR	1.25µM SOR	1.25µM SOR	SOR 1.25 µM 100 µM Naproxen	SOR 1.25 µM 100 µM Naproxen	SOR 1.25 µM 100 µM Naproxen	SOR 1.25 µM 200 µM Naproxen	SOR 1.25 µM 200 µM Naproxen	SOR 1.25 µM 200 µM Naproxen	SOR 1.25 µM 400 µM Naproxen	SOR 1.25 µM 400 µM Naproxen	SOR 1.25 µM 400 µM Naproxen
2.5 µM SOR	2.5 µM SOR	2.5 µM SOR	SOR 2.5 µM 100 µM Naproxen	SOR 2.5 µM 100 µM Naproxen	SOR 2.5 µM 100 µM Naproxen	SOR 2.5 µM 200 µM Naproxen	SOR 2.5 µM 200 µM Naproxen	SOR 2.5 µM 200 µM Naproxen	SOR 2.5 µM 400 µM Naproxen	SOR 2.5 µM 400 µM Naproxen	SOR 2.5 µM 400 µM Naproxen
5 µM SOR	5 µM SOR	5 µM SOR	SOR 5 µM 100 µM Naproxen	SOR 5 µM 100 µM Naproxen	SOR 5 µM 100 µM Naproxen	SOR 5 µM 200 µM Naproxen	SOR 5 µM 200 µM Naproxen	SOR 5 µM 200 µM Naproxen	SOR 5 µM 400 µM Naproxen	SOR 5 µM 400 µM Naproxen	SOR 5 µM 400 µM Naproxen
10 µM SOR	10 µM SOR	10 µM SOR	SOR 10 µM 100 µM Naproxen	SOR 10 µM 100 µM Naproxen	SOR 10 µM 100 µM Naproxen	SOR 10 µM 200 µM Naproxen	SOR 10 µM 200 µM Naproxen	SOR 10 µM 200 µM Naproxen	SOR 10 µM 400 µM Naproxen	SOR 10 µM 400 µM Naproxen	SOR 10 µM 400 µM Naproxen

Figure 2.3 1: Template for SRB Assay.

After 72 hours of incubation, cells were washed with 1x PBS and then fixed by adding 50 µl of 10% TCA into each well and kept at +4°C in the dark for at least 1 hour. Then, fixed cells were washed with ddH2O 3 times. When the wells were completely dried, SRB dye was prepared as a 0.4% SRB in %1 acetic acid solution and 50 µl of SRB dye was added to each well to be incubated at RT in the dark for 15 minutes. After staining, wells were washed with 100 µl of %1 acetic acid at least 3 times. Then, SRB dye was solubilized in 100 µl of 10 mM Tris-base with gently shaking at RT temperature for 15 minutes. Absorbance values were obtained at 515

nm using a microplate reader. Values were compared and normalized to DMSO and percent inhibition values of each condition were generated.

2.3.2 Synergyfinder Tool

To assess whether drug combinations were synergistic or not, the *''Synergyfinder''* tool (https://synergyfinder.fimm.fi/synergy/synfin_docs/) was utilized which is an interactive tool for assessing synergism between the drug pair. It reveals that drugs are either synergistic or antagonistic. It is accomplished by comparing the observed drug combination response coming from our experiments against the expected drug response, which is calculated using different synergy scoring models. Synergyfinder used all the synergy scoring models; HSA, Loewe, Bliss, and ZIP to quantify the degree of synergism. Each model has its assumption and considering the interaction pattern of the drugs; the suitable scoring model was selected. Synergy score analysis was performed in the ZIP model which states that the drug has zero interaction; in other words, the combination of the drugs neither affects their dose-response curves nor has a very minimal effect.

2.3.3 Real-Time Cell Analyzer System

To monitor cell growth in real-time, background reading was performed by adding 50 µl of DMEM into each well of 96-well E-plate. Then, Mahlavu and Huh7 cells were seeded 1500 cells/well and 2500 cells/well in 100 µl DMEM, respectively. E-plate was placed on its platform ''xCELLigence station'' inside a 6% CO_2 , 37 °C incubator. The next day, once the Cell Index (CI) values reached 0.6-0.8, the proliferation step was aborted and cells were treated with the drugs in 150 µl DMEM in triplicates. Then, a fast drug response reading was initiated in which CI values were recorded every 10 minutes. This step was followed by a long-term drug response step where CI values were recorded every 30 minutes for the following 48 hours. CI values were exported and normalized to time-zero CI values (TZ) and then

percent inhibition values for each drug treatment were calculated compared to the DMSO group.

2.3.4 Pathway Analysis

2.3.4.1 Data Collection

The transcriptomic data for Naproxen was obtained from Connectivity Map (CMap) LINCS 2020-level5 data, and transcriptomic data for Sorafenib was obtained from E-MTAB-7847 RNAseq data.

2.3.4.1.1 Differentially expressed gene (DEG) collection

Sorafenib RNA sequencing data has values for 25146 genes while CMap LINCS-level5 data has values for 12327 genes. Among those, 10679 genes are common in both data sources and only common genes were used for further analysis. Differential expression in the network reconstruction studies is defined such that genes with logFC values above or equal to +2 are up-regulated while genes with logFC values below or equal to -2 are down-regulated.

For Sorafenib RNA sequencing Data, log2FoldChange values and corresponding p-values were used which are already available in the data source. Genes with $p<0.001$ are collected for up-and-down-regulated genes.

Within the CMAP LINCS-level5 data, transcriptomic data of Naproxen treatment has three replicates for the same treatment conditions. log2FoldChange values were calculated from the mean of these replicates. Using the calculated logFC values, up-regulated and down-regulated genes were collected.

2.3.4.2 Network Reconstruction

Gene list with their prizes which include differentially expressed genes and drug targets were uploaded in the Omics Integrator tools (Tuncbag et al., 2016). Drug targets were manually collected from CMAP Drug repurposing tool. The pipeline was shown in Figure 2.3.2. Prizes of differentially expressed genes were defined by the absolute values of corresponding logFC values. Prizes of drug targets were set a constant value that will be the highest among the others to force the algorithm to include the drug targets in the final optimum network.

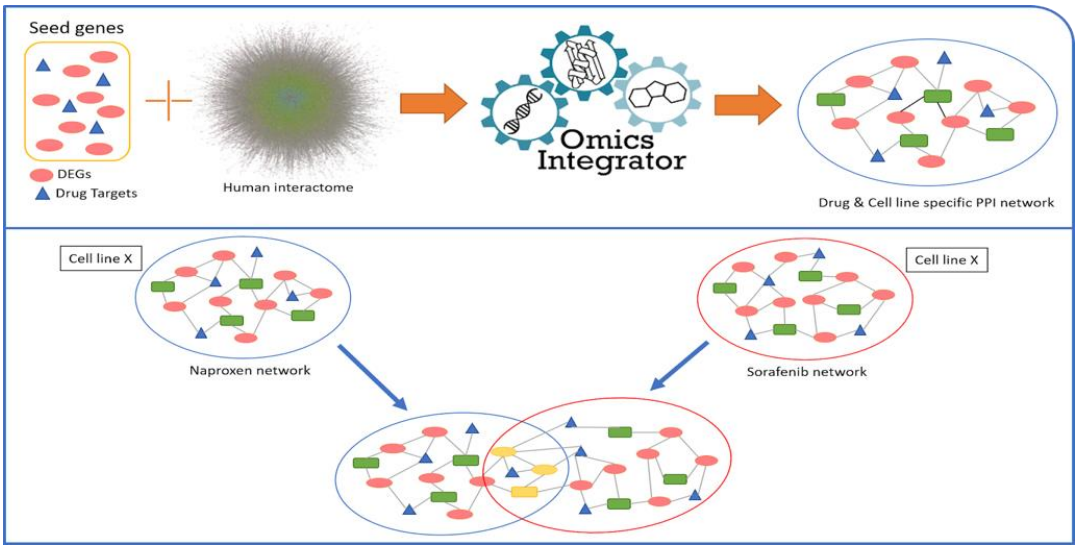

Figure 2.3 2: Pipeline for network reconstruction

2.3.5 Annexin-V/PI staining

Huh7 (60.000 cells/well) and Mahlavu cells (30.000 cells/well), were seeded in six-well plates. The next day, cells were treated with a selected dose of sorafenib, naproxen, or doxorubicin. After 72h, both attached and detached cells were collected into falcon tubes. 80 µl of aliquots of each sample were transferred into Eppendorf tubes and counted by flow cytometry. The total number of cells was determined in each sample and 1X assay buffer was added accordingly. In the meantime, samples were centrifuged at 1500 rpm for 5 minutes, washing was performed with 1x PBS 2

times. Pellets were resuspended with Annexin-V Apoptosis detection kit's 1X assay buffer (100 µl/10^6 cells, which was supplemented with 1% of FBS). Then cells were stained with 1 µl of PI and FITC followed by 15 minutes of incubation at RT in the dark. Before flow cytometry analysis, 400 µl of 1X binding buffer was added to each sample. Cells that were stained with both PI and FITC indicated late apoptotic cells.

2.3.6 Immunohistochemistry staining with Hoechst 33258 fluorescent dye

Huh7 and Mahlavu cells were seeded in six-well plates with coverslips for each time point 24h, 48h, and 72h, as indicated in Table 2.3.2. The next day, the old media was refreshed with the selected dosage of Naproxen and Sorafenib. After 24h, 48h, and 72h hours, old media were aspirated, wells were washed twice with 1X PBS and fixed with cold 100% methanol (stored at -20°C) for 10 minutes at RT. Methanol was aspirated, and cells were washed with 1XPBS 2 times. For the staining of cell nuclei, Hoechst 33258 (300 µg/ml) was diluted with 1X PBS (400 µl/well) to prepare 1 µg/ml stain (%v/v). Cells were incubated with Hoechst stain at RT for 5 minutes in the dark, followed by washing with ddH_2O. To remove excess dye, the destaining process was performed with incubation for 10 minutes with ddH_2O at RT in dark. Finally, tiny drops of glycerol were added to mount the coverslip on the slides, and cell nuclei were visualized under fluorescence microscopy.

Table 2.3.2: Number of cells (cells/well) seeded for each incubation time in six-well plates

Cell line	24h	48h	72h
Huh7	180.000	90.000	60.000
Mahlavu	90.000	45.000	30.000

2.3.7 Western Blot

2.3.7.1 Sample Preparation

Huh7 (1.200.000 cell) and Mahlavu (600.000 cell) were seeded in 15 mm cell culture dishes. Next day, the medium was refreshed with the 12 ml media that contain the selected dosage of Naproxen and Sorafenib. After 24h of treatment, cells were collected into 50 ml of falcon tubes with 1X PBS on ice via scraping. Cells were centrifuged at 2000 rpm for 6 minutes at +4°C and washed with 1X PBS two times. After removing the supernatant, cells were either stored at -80°C or directly used for protein extraction.

2.3.7.2 Crude protein extraction

NP-40 lysis buffer (described in 2.2.4) was added (20 to 100 µl) according to the pellet size. Pellet was resuspended with the required amount of lysis buffer and incubated on ice for 30- 45 minutes. Samples were vortexed every ten minutes for 10 seconds. The lysates were centrifuged for 20 minutes at 13.000 rpm at +4°C. Supernatants, which contained our proteins of interest, were collected into new Eppendorf tubes. It is used directly to quantify the amount of protein in the sample or stored for the short term at -20°C or long- term at -80°C.

2.3.7.3 Protein Quantification by Bicinchoninic Acid (BCA) Assay

BSA (Serum Albumin) protein (20mg/ml stock) was prepared as 2mg/ml, 1mg/ml, 0.5mg/ml, 0.25mg/ml, and 0.125mg/ml with filtered ddH_2O. BCA Assay kit (B9643) procedure was followed to quantify protein concentration in each sample. Samples were prepared as 1:20 dilution with ddH_2O. ddH_2O was also used as blank. Finally, 25 µl from each sample, blank solution, and BCA protein with different dilutions were mixed with a 200 µl of BCA working reagent (reagent A (X) and reagent B

(50x); 1:50) on 96 well plates. Plates were incubated for 30 minutes at 37°C and were read at 562 nm. Blank OD values were subtracted from the BCA protein and samples. Blank-corrected OD values of BCA protein were used to generate the standard curve, and each sample protein concentration was determined according to this curve with the formula y=ax+b; (sample OD=y, x=protein concentration of samples.

2.3.7.4 Gel loading and Running

10 well or 15 well comb stain-free gel were used for western blot experiments. 40 µg of protein in 25 µl or 30 to 50 µg protein in 12 µl were loaded for each gel, respectively. Before SDS-PAGE electrophoresis, each sample was prepared in a mixture that contain the protein, 1x Laemmli buffer, DTT and ddH_2O. The samples were mixed well by pipetting or quick vortexing and incubated at 95°C for 7 minutes to denature the proteins. Then, samples were quickly transferred to the ice and were spun down subsequently. In the meantime, 1X Tris-Glycine running buffer was prepared with cold dH_2O, and a cassette was established in the tank. Samples and ladder (Chameleon Duo, Licor) were loaded into respective wells, and running was performed for 20-30 minutes with 150V.

2.3.7.5 Semi- dry transfer

Low-fluorescence (LF) PVDF membranes were used for the fluorescence imaging system. Membranes were soaked in methanol for 30 seconds and rinsed with ddH_2O then soaked into transfer buffer for 2 minutes before transfer for activation. In the meantime, transfer packs were placed in transfer buffer for 2 minutes to ensure packs were completely wet. A sandwich was prepared and placed into the Trans blot transfer device. Transfer was done for around 7 minutes.

2.3.7.6 Total Protein Staining

After the proteins were transferred to the membrane, it was dried for 10 minutes in the oven at 37°C for better protein retention. The membranes were thoroughly dried, rehydrated with methanol for 30 seconds, gently shaken with TBS for 5 minutes and rinsed with ddH_2O. Then, LI-COR's revert Total protein staining protocol was followed. Membrane was gently shaken with Revert 520 Total Protein Stain for 5 minutes and washed 2 times for 30 seconds with Licor's wash solution and rinsed with ddH_2O. The gel image was taken using the LI-COR-Odyssey system using only the 700 channel. To remove total protein staining, membranes were incubated with Revert destaining solution with gentle shaking for up to 10 minutes at RT.

2.3.7.7 Blocking

LI-COR's Odyssey Blocking (TBS) buffer was used to block the membrane either 1 hour at RT or overnight at +4°C with gentle shaking.

2.3.7.8 Primary and the Secondary antibody incubations

The primary antibody was prepared in their blocking solution with 0.2% Tween20. The membrane was incubated with the primary antibody for either two hours at RT or overnight at +4°C with gentle shaking. Then the membrane was washed with 1x TBS-T for 5 minutes three times with shaking. A secondary antibody was also prepared in their blocking solution with 0.2% Tween20 and %0.01 SDS. The incubation time for the secondary antibody was 1 hour at RT in the dark with gentle shaking. The washing step was the same as the primary antibody washing. Then the membrane was placed in a container with 1X TBS. The image was taken in LI-COR's Odyssey CLx imaging system.

2.3.7.9 Visualization of the membrane

Images were taken in both 700 and 800 channels with the highest quality in the LI-COR Odyssey imaging system.

2.3.8 Gene expression analysis

2.3.8.1 Primer Design for qRT-PCR

The coding sequences (CDS) of the gene of interest were found on NCBI (National Center for Biotechnology Information) website: https://www.ncbi.nlm.nih.gov/gene. NCBI Primer Blast was used for the design of the primer. The following criteria were met for each primer design; primer length was around 18-22 bp, GC content of 40-60%, and the melting temperature was around 60°C (with a max. 2°C difference between primer pairs). Another essential criterion for primer design was to ensure that the amplified regions must span an exon-exon junction and that the product size was 70-200 bp. Primer pairs used in this study were listed Table 2.1.8.

2.3.8.2 Sample Collection

Huh7 and Mahlavu were seeded in 10 mm cell culture dishes for 24h and 48h with an indicated cell number shown in table 2.3.3. Next day, cells were treated with the selected drugs. After 24h and 48h of incubation, old media was aspirated, cells were collected via trypsinization and centrifuged at 300g for 5 min. Then, cells were washed 2 times with 1X PBS. The supernatant was removed and the cell pellet was stored at -80°C or was immediately used for RNA isolation.

Table 2.3.3: Number of cells (cells/well) seeded in 10mm dishes for different time points

Cell line	24h	48h
Huh7	600.000	300.000
Mahlavu	300.000	150.000

2.3.8.3 Total RNA extraction

Qiagen's RNeasy Mini kit was used to perform RNA isolation, and manufacturing protocols were followed. According to pellet size, buffer RLT was added 350-600 µl, and the pellet was syringed to homogenize the pellet. 1 volume of Ethanol was added to the mixture and pipetted well. Then 350 ul of the sample was transferred to the RNeasy spin column. Samples were centrifuged for 15 seconds at 8000 x g, and the flow-through was discarded. 700 µl Buffer RW1 was added onto each spin column and centrifuged for 15 seconds at 8000 x g; flow-through was discarded. 500 µl of Buffer RPE was added to the spin column and centrifuged for 15 seconds at 8000 x g then the flow-through was discarded. 500 µl of Buffer RPE was added to the spin column and centrifuged for 2 minutes at 8000 x g. Then the spin columns were placed in a 1.5 ml collection tube, and 20 µl of RNeasy-free water was added directly to the middle of the spin column and centrifuged for 1 minute. RNA specimen was eluted to 1.5 ml collection tube and measured in nanodrop for the concentration of RNA and its quality considering the ratio of A260/A280, A260/A230. RNA samples were treated with DNAse to avoid genomic DNA contamination, DNA-freeTM DNA Removal Kit was followed according to the manufacturer's instructions. To confirm the removal of genomic DNA, conventional PCR was performed with GAPDH primer, and it was repeated until genomic DNA contamination disappeared.

2.3.8.4 cDNA synthesis

cDNA synthesis was performed with RevertAid First Strand cDNA synthesis kit (Fermentas). 1 µg of total RNA was used for the first strand cDNA synthesis. The required volume for each RNA specimen was determined, and 1 µl of oligo dT was added. Then the total volume was completed to 12 µl with RNAse-free water, incubated in a thermal cycler for 5 minutes at 65 °C. 10 mm dNTP, Ribolock, and 5x buffer RevertAid M-MulV RT enzyme were mixed well, and 8 µl was transferred to each sample to complete final volume to 20 µl. Incubation was started for 5 minutes at 25°C and 60 minutes at 42°C in the thermal cycler. The amount of cDNA that was synthesized was determined in nanodrop. cDNA was aliquoted (100ng/ µl) and stored at -20°C.

2.3.8.5 Expression analysis-qPCR

Real-time quantitative PCR reactions were performed in triplicates for each gene of interest. 200 ng/µl cDNA was used to set up the reaction. Since cDNA was aliquoted as 100 ng/ µl, 2 µl of cDNA were used. The PCR Master mix contained 2 µl of cDNA, 0.5 µl of both reverse and forward primers, 5 µl of SYBR Green, and 2 µl of RNase-free water to complete 10 µl of reaction setup. The following cycles were used to run the reaction; initial denaturation for 10 min at 95 °C, 45 cycles amplification for 10 sec at 95°C followed by 10 sec at 61°C and 10 sec at 72°C, and melting for 10 sec at 95°C followed by 65°C for 60 sec and 1 sec at 97°C. To calculate primer efficiency, cDNA for each gene of interest was diluted as 1:15, 1:30, 1:60. The standard curve (Cycle threshold (Ct) vs. log of starting quantity) was plotted in Light Cycler® 96 Real-Time PCR System. Then, relative expression values were calculated with this information. Cq values were created by the system and transformed into relative expression values within this formula $2^{-\Delta\Delta Ct}$. The relative expression between the experimental and the control group was calculated

with the formula R = (Etarget)ΔCqtarget(control-sample) /(Eref) ΔCqref(control-sample).

2.3.8.6 Agorose Gel electrophoresis

2% Agarose was dissolved in TAE buffer in a microwave for around 2-3 minutes until it was completely dissolved; every 25 ml of TAE buffer required 1 µl of EtBr. After adding EtBr, it was poured onto a gel casting apparatus for polymerization. PCR products were mixed with 6X loading dye before the sample's loading onto the gel. In the meantime, BioLabs 50 bp DNA ladder was prepared at a 1:1 ratio; 1 µl of gel loading dye and 1 µl of DNA ladder were mixed with the addition of 4 µl of TAE buffer to complete the final volume of 6 µl.

2.3.9 Cell Cycle analysis with PI staining

Huh7 (90.000 cells/well) and Mahlavu (45.000 cells/well) were seeded into six-well plates. The next day, old media was refreshed with new media containing a selected dosage of Sorafenib and Naproxen. After 48h, all the attached and detached cells were collected to the falcon and centrifuged at 1800 rpm for 5 minutes at 4°C. Pellet was washed with 1X cold PBS and fixed with 1 ml cold 70% ethanol for at least 3 hours at -20°C. After fixation, 1X cold PBS is added to each falcon and centrifuged at 1800 rpm for 5 minutes at 4°C to remove ethanol. Pellets were resuspended and incubated with 50 µl RNAse A at 37°C for 15 minutes. After RNAse incubation, 200 µl of PI was added to each Eppendorf and incubated for 30 minutes at 37°C. 100 µl of 1X PBS was added before flow cytometry analysis.

2.3.10 Statistical Analysis

All experiment was performed with at least three biological replicates, and each experiment was designed to contain three technical replicates. GraphPad Prism 8

was used to draw graphics and perform statistical analysis. One-way ANOVA and the student-t test was used to determine the statistical significance between the groups. P-value <0.05 is considered statically significant.

CHAPTER 3

RESULTS

Firstly, FDA-approved anti-inflammatory drugs, including Aspirin, Naproxen, Ibuprofen, and Flurbiprofen, were tested with Sorafenib, Lenvatinib, and Regorafenib on HCC cell lines to investigate whether they are synergistically interacting or not. Secondly, with the selection of synergistically interacting drug pairs, network analysis of each drug was performed to explore the possible anti-cancer activity mechanism of the drug combination. Signaling pathways modulated by the two different drug networks were revealed upon the network analysis; The pathway enriched in both drugs has been supported and demonstrated by *in vitro* methods in HCC cell lines. Moreover, the shared gene from the network in both drugs is analyzed further. Lastly, the activity of most-deregulated -mutated pathways in HCC, including AKT were studied in terms of changes in protein and gene expression level.

3.1 Selection of synergistically interacting anti-inflammatory drugs and anti-cancer drug pairs in hepatocellular carcinoma cell lines

Aspirin, Naproxen, Ibuprofen and Flurbiprofen were combined with Sorafenib, Lenvatinib, and Regorafenib and tested on Mahlavu and Huh7 cell lines by NCI-SRB assay to find out their interaction pattern in terms of synergism. Percent inhibition of each dose of combination was found and synergistic interaction was investigated accordingly by using Synergyfinder tool and R programming. Among different NSAIDs and HCC drugs, naproxen and sorafenib combination were found to be synergistically interacting. Percent inhibition of the Mahlavu and Huh7 cells was increased when the drugs were applied together. (Figure 3.1A) and (Figure

3.1B)**,** respectively. The synergy score on HCC cell lines was calculated by Synergy finder as Zero Interaction Potency (ZIP) and it was 16.142 for Mahlavu and 16.482 for Huh7 cells.

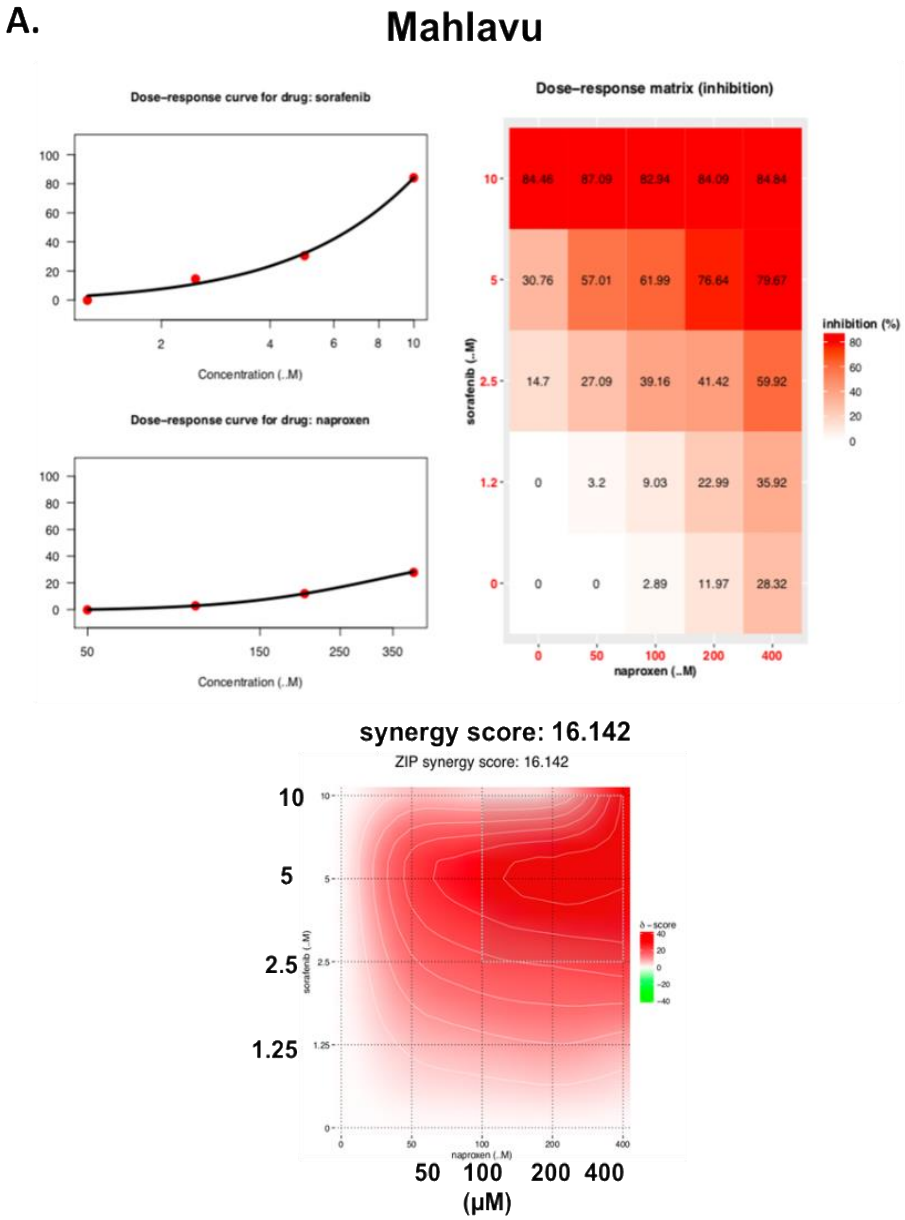

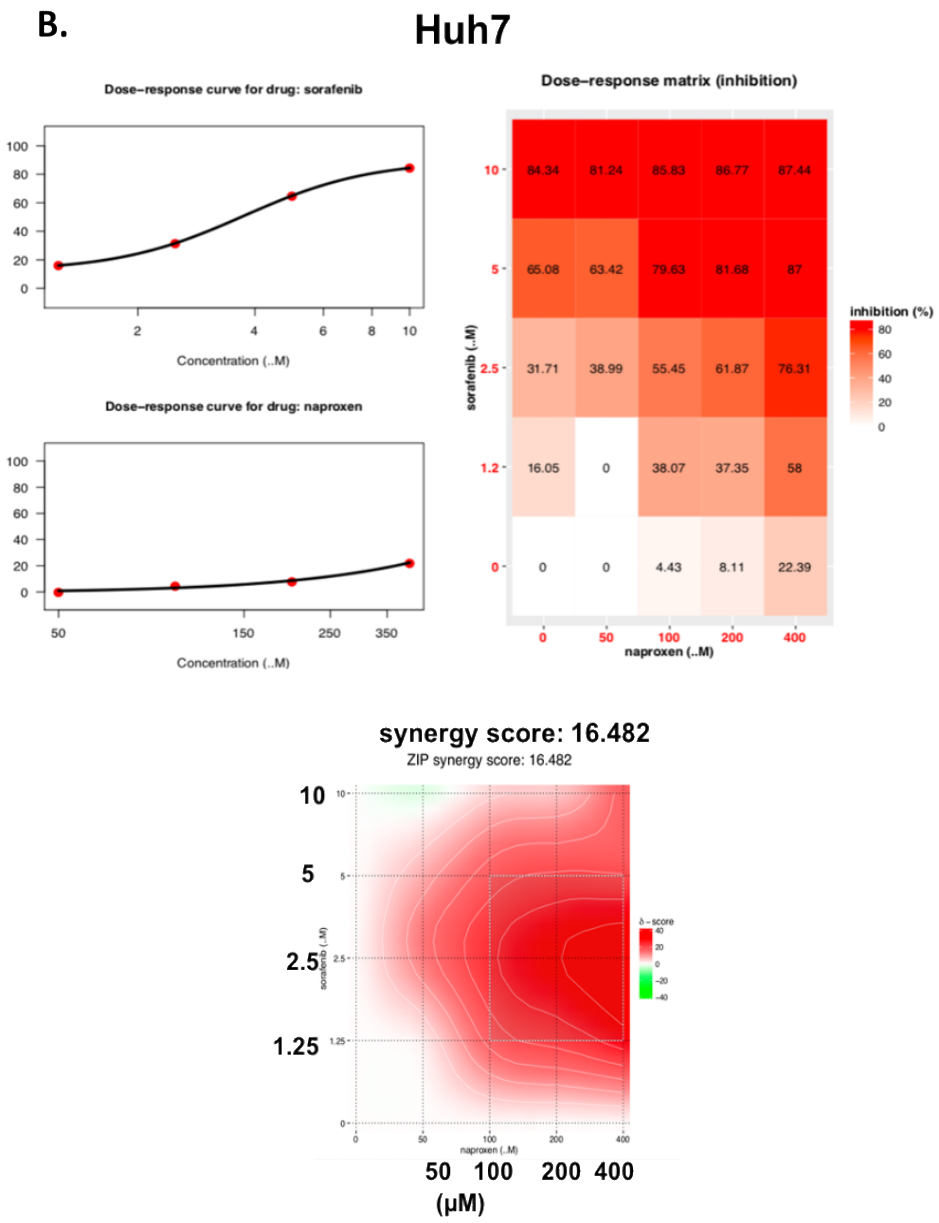

Figure 3. 1 Naproxen and Sorafenib show synergistic interaction in HCC cell lines. Dose-response curve and matrix were generated in 72h treatment of Sorafenib and Naproxen by NCI-SRB assay **A.** synergy score were found as 16.142 in Mahlavu and **B**. 16.482 in Huh7 cell lines. Most synergistic areas were shown as dark red.

3.1.1 Effect of other combinations in HCC cell lines

NSAIDs, including aspirin, flurbiprofen, and ibuprofen combined with sorafenib, Lenvatinib, and Regorafenib, did not show synergistic interaction in HCC cell lines such as Mahlavu and Huh7. Sorafenib combined with either aspirin, flurbiprofen, or ibuprofen did not display synergistic interaction in Mahlavu and Huh7 cells (Figure A.1A). Lenvatinib combined with the same drugs aspirin, ibuprofen, flurbiprofen and naproxen also did not show synergistic interaction in Mahlavu (Figure A.1B) It was found that Lenvatinib is antagonistically interacting with each NSAID. Lastly, Regorafenib was tested on Mahlavu cell line with the combination of aspirin and naproxen that did not possess synergism (Figure A.1C). Therefore, among the combinations of different NSAIDs with HCC drugs, Naproxen and Sorafenib were found to be synergistically interacting in HCC. NCI-SRB assay was used to assess percent inhibition, and the *synergyfinder* package in R programming was used to calculate the ZIP synergy score.

3.1.2 Effect of combination in normal like fibroblast cells

To investigate the effect of synergism on normal-like cells, naproxen and sorafenib combination was tested on MCF12A cells. The synergy score was 11.328 (Figure A.2), smaller than Huh7 and Mahlavu cell lines. Therefore, the degree of synergism was considered not effective as cancer lines

3.1.3 Cytotoxic effect of the selected concentration of naproxen and sorafenib combination against HCC cell lines.

Considering the most synergistic area that was shown in (Figures 3.1A and 3.1B) synergistic concentrations of Naproxen and Sorafenib were selected accordingly. It

has been shown that selected concentrations of the drugs significantly decreased cell viability compared to other groups in Mahlavu and Huh7 cells (Figure 3.1.1).

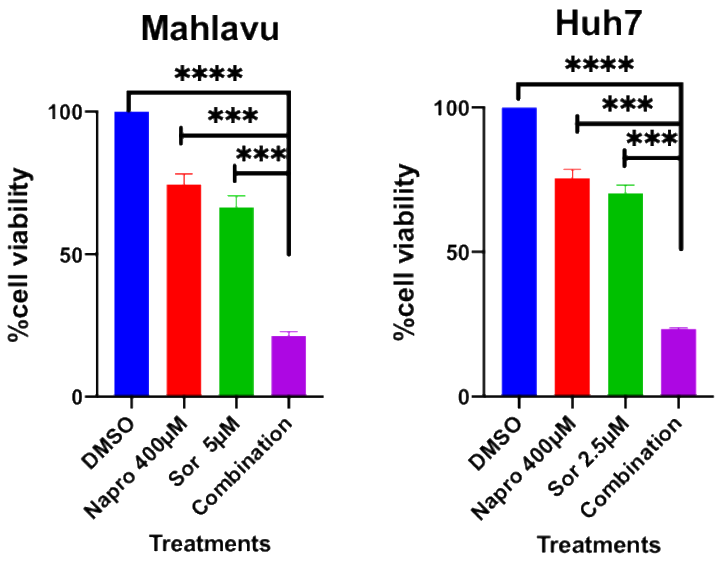

Figure 3.1. 1 The Selected synergistic concentration of Sorafenib and Naproxen combination decreases cell viability against HCC cell lines. Cell viability of Mahlavu and Huh7 was assesed by NCI-SRB assay after 72h of treatment with Sorafenib and Naproxen. One-way ANOVA is applied to determine significance.

3.1.1 Observation of real-time cell proliferation curve of sorafenib and naproxen against HCC cell lines

RT-CES system was utilized to monitor the cell growth of Mahlavu and Huh7 cells treated with Sorafenib and Naproxen. The concentration of Sorafenib and Naproxen was determined by NCI-SRB assay results. DMSO was used as vehicle control. Naproxen and Sorafenib combination induced dose-dependent inhibition of cell growth in HCC cell lines. The significance of drug combination disappears when 100 μM naproxen is combined with either 2.5 μM or 5 μM sorafenib. Other combinations significantly reduced cell growth compared to the other groups. (Figure 3.1.2)

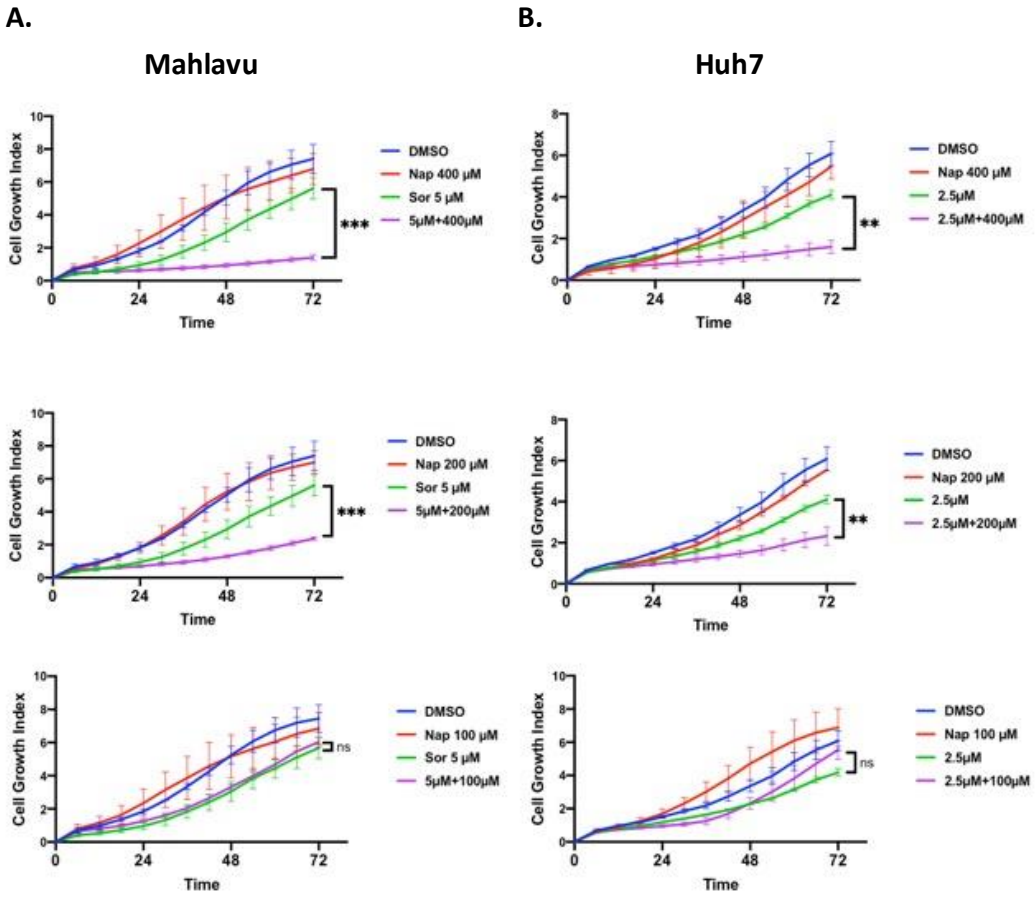

Figure 3.1. 2 Real-time cell growth analysis of HCC cells treated with selected concentrations of the drugs. The growth curves of Mahlavu (A) and Huh7 (B) are represented in 72h. Experiments were performed as three independent replicates. One-way ANOVA was applied to determine the significancy of the combination compared to DMSO control.

3.1.2 The morphological changes of HCC cells upon drug combination

Huh7 and Mahlavu cells treated with selected concentrations of Sorafenib and Naproxen were observed under microscopy for 24h, 48h and 72h. The morphology of the cells were shown in Figure 3.1.3. When drugs were applied together, cells became stressed and the number of unattached cells increase compared to single drug treated groups.

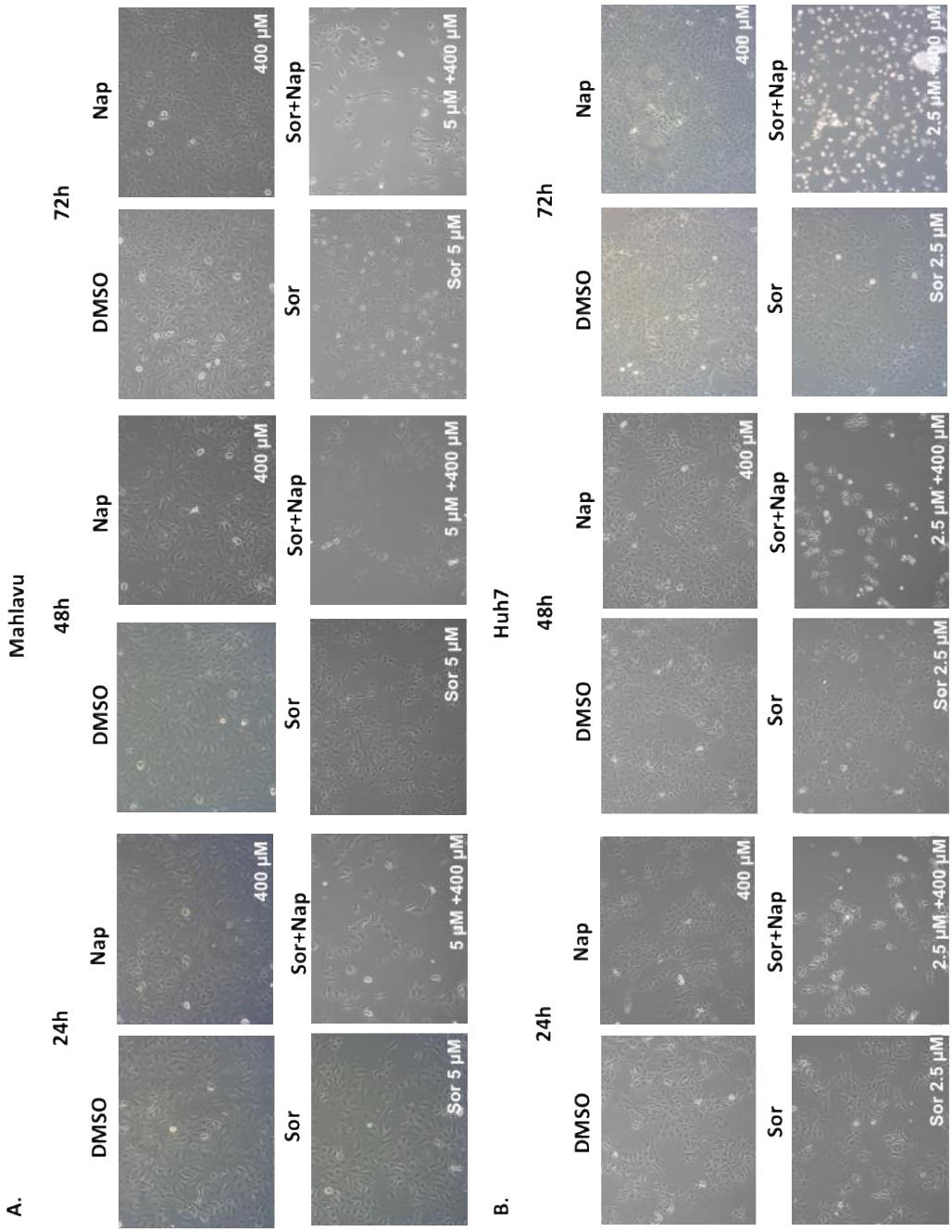

Figure 3.1. 3 Morphological changes of Mahlavu and Huh7 cells in different time points. Mahlavu (A) and Huh7 cells (B) were treated with indicated concentrations of drugs for 24,48, and 72 hours. Images were taken under light microscopy with 20X magnification.

3.2 Network Analysis of Sorafenib and Naproxen

In order to investigate the pathways implicated in either sorafenib or naproxen-treated HCC cells, we used publicly available transcriptomic data sets of Sorafenib from OMICSDI-EMTAB-7847 and Naproxen from CMAP database. Then, network analysis was performed to show not only the known mechanism of the drugs but also discover hidden mechanisms of Naproxen and Sorafenib.

3.2.1 Determination of differentially expressed genes of Naproxen and Sorafenib treated cells

The total number of 10.679 genes retrieved from Naproxen and Sorafenib gene expression data, was shown in Venn diagram. The number of common genes which are differentially expressed in both sorafenib and naproxen treated Huh7 was calculated and shown in Figure 3.2.1. It was found that few numbers of genes were common in Sorafenib and Naproxen treated Huh7 cells, compared to the total number of genes. Only 45 common genes were upregulated in both groups whereas only 30 common genes were downregulated for both Naproxen and Sorafenib-treated HCC cell lines.

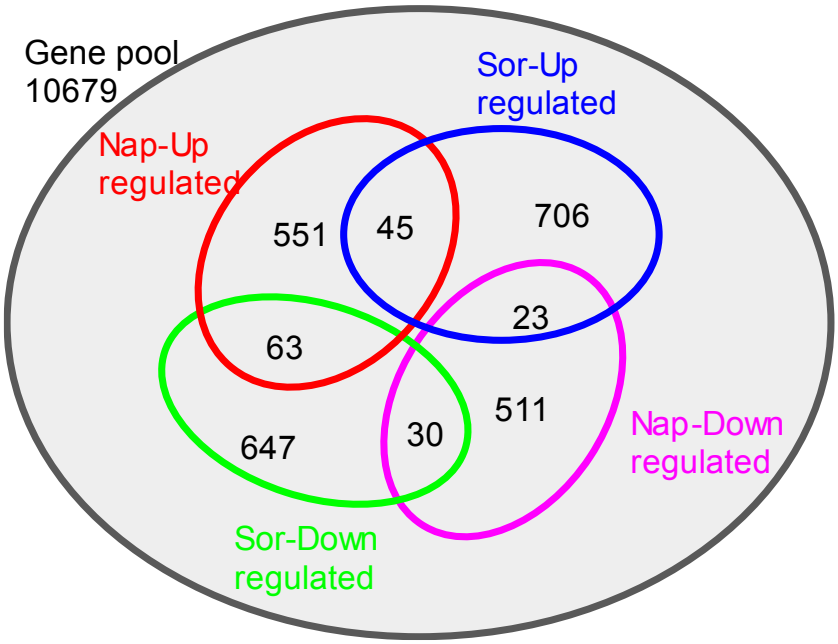

Figure 3.2 1 Venn diagram representation of differentially expressed genes in sorafenib and naproxen treated cells.

3.2.2 Network analysis of sorafenib and Naproxen in Huh7 cells

Network analysis revealed that Sorafenib and Naproxen modulate different pathways in Huh7. Apoptosis related genes were enriched in both networks which were labeled as red dots in the network (Figure 3.2.2). CAPN2 gene was found as the only gene that is common in both Sorafenib and Naproxen networks.

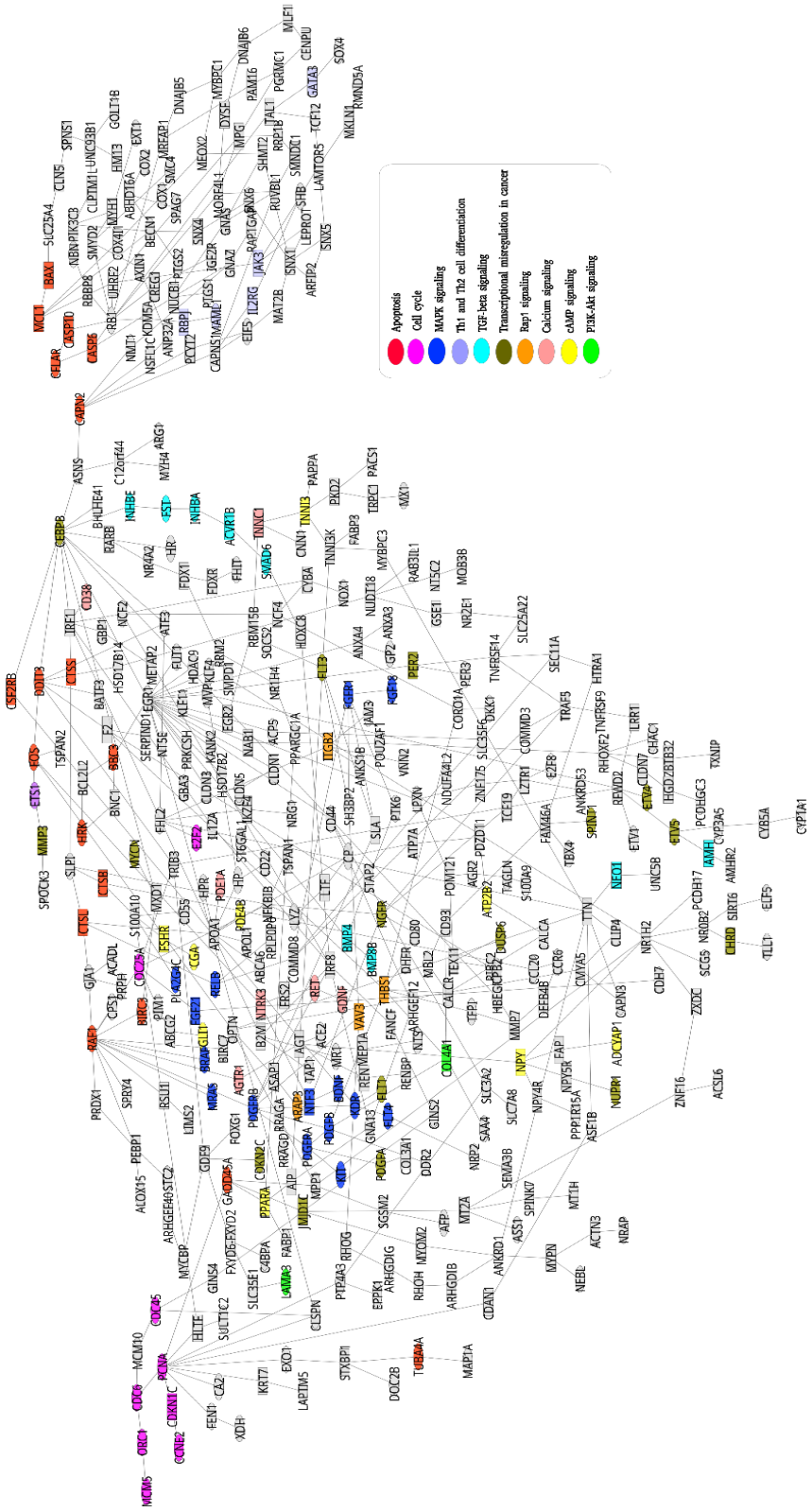

Figure 3.2 2 Network analysis of Sorafenib and Naproxen in HCC cell line.

3.2.3 Gene enrichment analysis in Sorafenib and Naproxen Network

Network analysis revealed that apoptosis pathway was enriched in both Sorafenib and Naproxen network (Figure 3.2.3). It implied that apoptosis can be implicated in drug combination since it is found to be enriched in both sorafenib and naproxen networks.

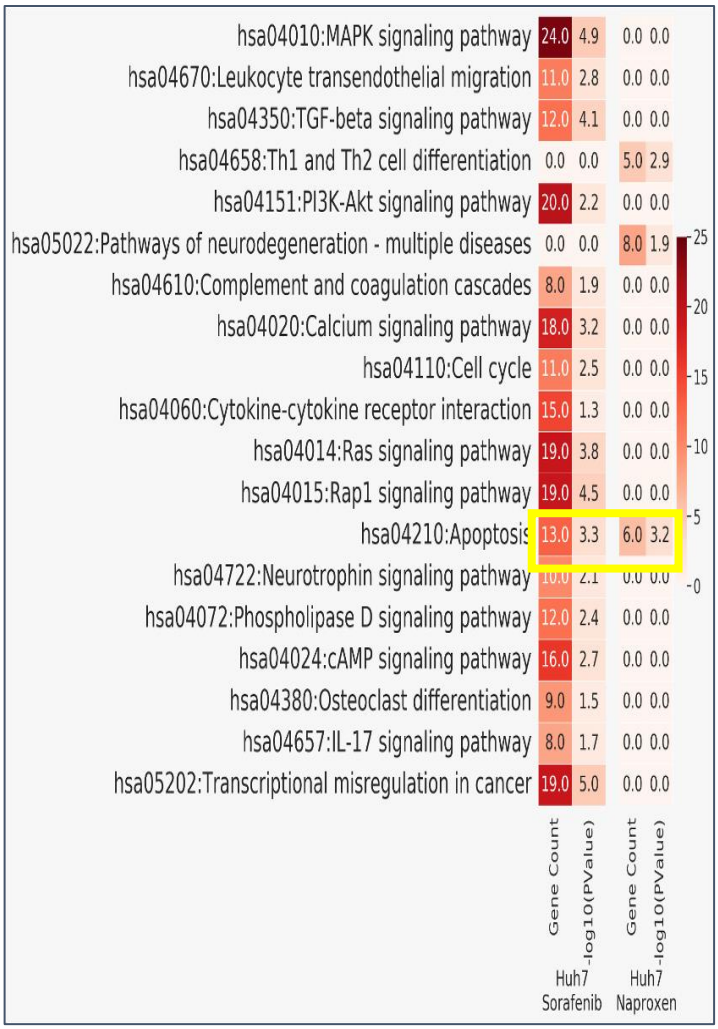

Figure 3.2 3 Representation of pathway enrichment result of Sorafenib and Naproxen in HCC cell line.

3.3 Sorafenib and Naproxen combination induce apoptosis in HCC cell lines

Since apoptotic cell death has some characteristic features such as chromatin condensation, nucleus fragmentation, formation of apoptotic bodies, or flip-flop motion of phosphatidylserine (PS) on the cell membrane, based on these specific features, there are commonly used methods for apoptosis detection. Apoptosis in HCC cell lines treated with sorafenib and naproxen were detected in Hoechst staining, Annexin-V/PI staining and also apoptosis signaling was studied in detail by observing changes in apoptosis mediator protein such as PARP, Caspase-8, Caspase-9, Bcl-$x_{S/L}$ and Cytochrome-c. Firstly, Hoechst 33258 staining was performed to show apoptosis at different time points (24h, 48h, 72h). Since Hoechst 33258 staining is a fluorescent dye that stains nuclei of fixed living cells, it is used to detect condensed nuclei and apoptotic bleb as an indicator of apoptosis. Figure 3.3.1 shows representative images of Hoechst staining in Mahlavu (Figure 3.3.1A) and Huh7 (Figure 3.3.1B) cell lines treated with either sorafenib and naproxen alone or with their combination. Fragmented DNA and apoptotic blebbing in combination were observed in 24h and becomes more apparent in 48h and 72h. Moreover, apoptotic blebbing was observed very minor in Mahlavu and Huh7 cells treated with either sorafenib or naproxen alone.

A.

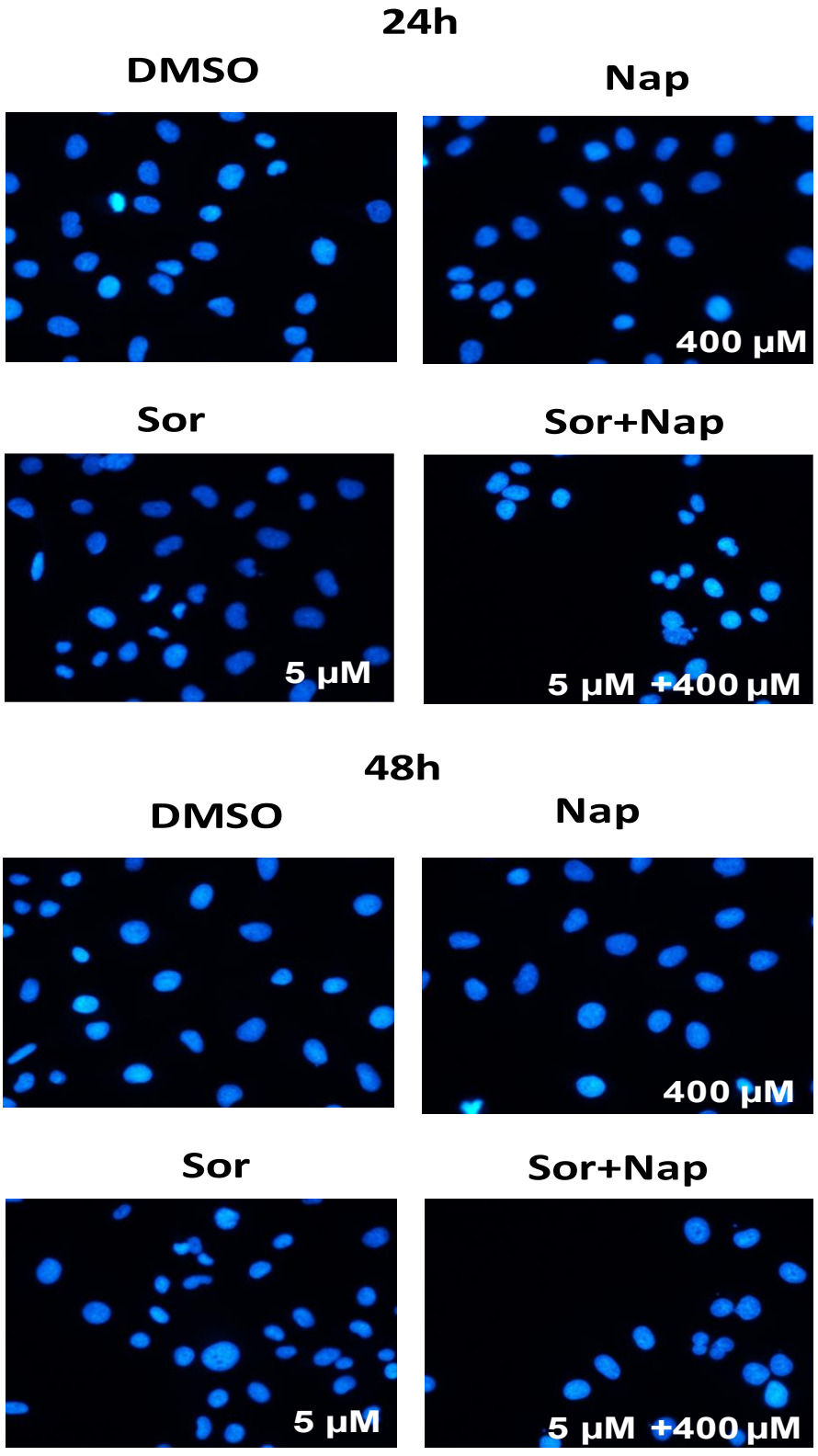
24h
DMSO
Nap
400 µM
Sor
Sor+Nap
5 µM
5 µM +400 µM
48h
DMSO
Nap
400 µM
Sor
Sor+Nap
5 µM
5 µM +400 µM

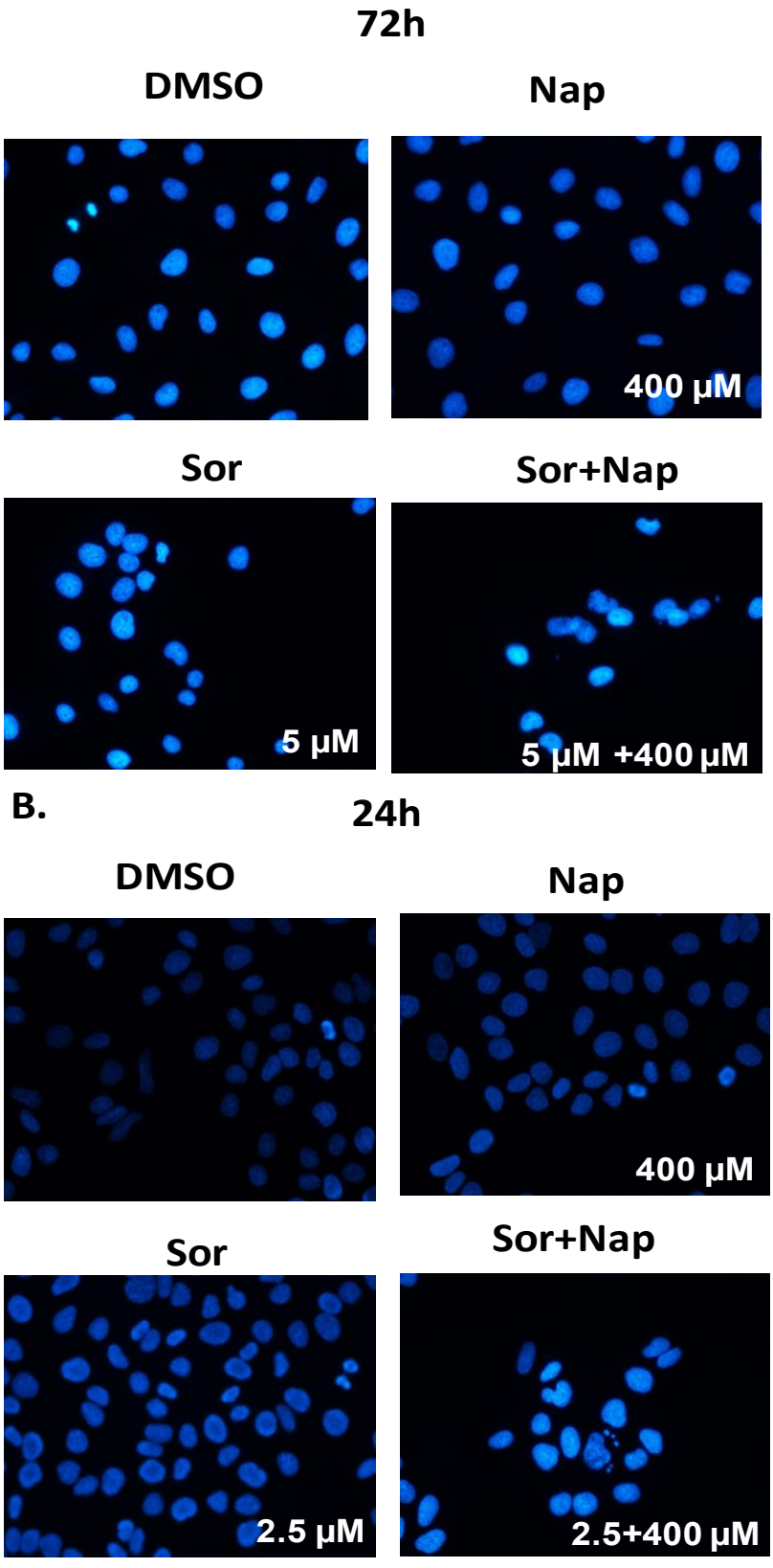
72h
DMSO
Nap
400 µM
Sor
Sor+Nap
5 µM
5 µM +400 µM
B.
24h
DMSO
Nap
400 µM
Sor
Sor+Nap
2.5 µM
2.5+400 µM

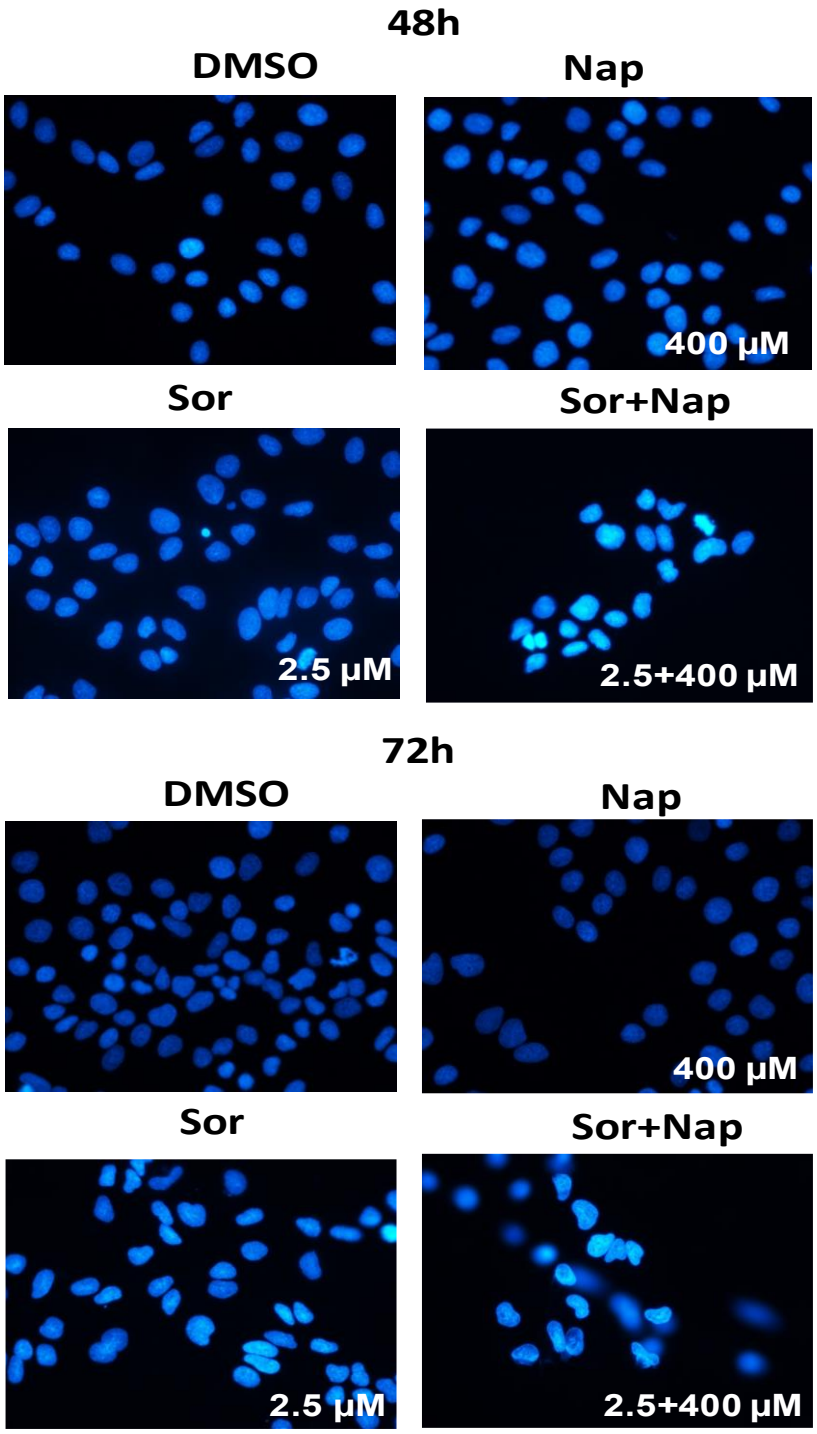

Figure 3.3. 1 Hoechst staining of HCC cells in 24h, 48h, and 72h of treatment. **A.**Mahlavu **B**.Huh7 cell treated with indicated concentrations. Images were taken under 40X magnification.

As mentioned, one other indicator of apoptosis is flip-flop motion of phosphatidylserine on the cell membrane, which could be detected by annexin/PI staining in flow cytometry. If cells were stained with only annexin-V, it indicates early apoptosis, whereas cell stained with both PI and annexin-V indicates late apoptosis. Figure 3.3.2 shows Mahlavu and Huh7 apoptosis analysis in flow cytometry. Neither 5 µM of Sorafenib nor 400 µM Naproxen could not increase the apoptotic population in Mahlavu cells, whereas when Mahlavu is treated with both drugs, annexin-V and PI-positive cell populations (Q3) significantly increased. (Figure 3.3.2A). Although Huh7 cells treated with 2.5 µM sorafenib increased apoptotic cell population and 400 µM of naproxen did not induce apoptosis, the combination of the drugs significantly increased the apoptotic cell population. (Figure 3.3.2B). Doxorubicin is a well-known chemotherapeutic drug for inducing apoptosis and was used as a positive control. Apoptosis analysis of sorafenib combined with 200 µM naproxen was shown in (Figure A.3)

A.

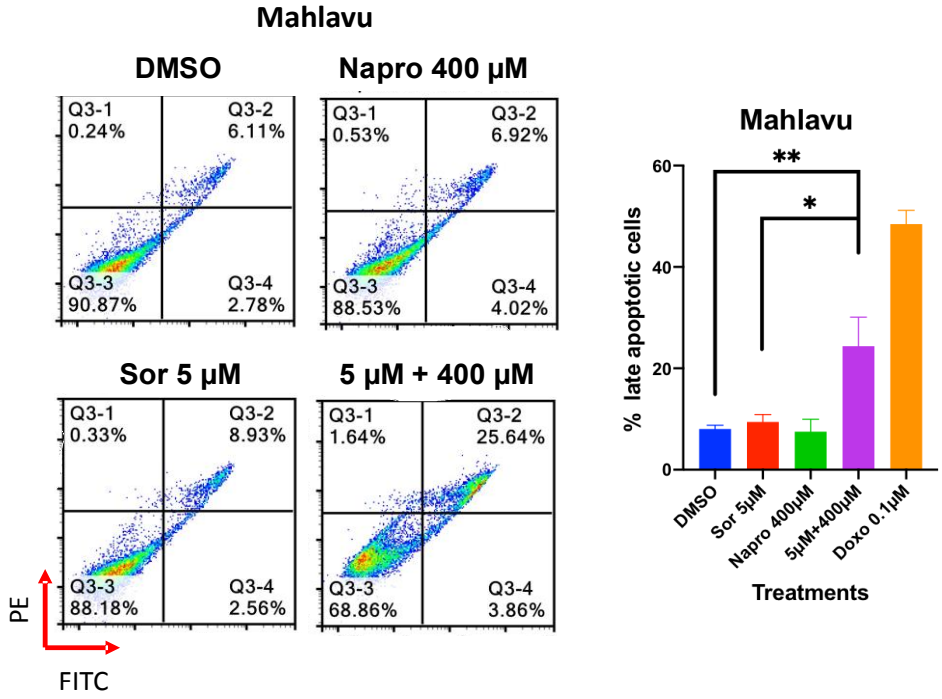

B.

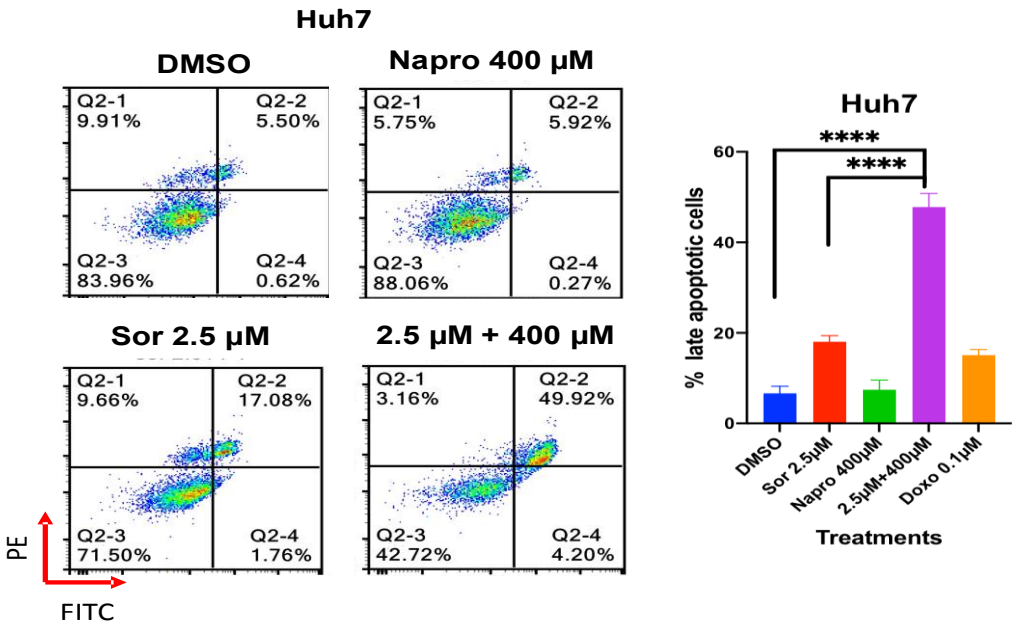

Figure 3.3. 2 Flow cytometry analysis of Annexin-V/PI staining and bar graph representation of late apoptotic cells. Cells were stained with Annexin-V and PI after 72h of treatment. Q2-1 represents necrotic cells, Q2-2 shows the population that was positive for both PI and annexin-V and which represents late apoptotic cells, whereas Q2-4 indicates early apoptotic cells that were positive for only Annexin-V, cell membrane remains intact, PI can not enter inside the cell. One-way ANOVA was applied to determine significance.

Moreover, western blot was performed to show changes in the expression of apoptotic proteins such as PARP, caspase-9, caspase-8 and BCL-xL (S-18) and BCL-xs(S-18) and cytochrome-c in HCC cell lines. Figure 3.3.3 shows western blot analysis of apoptosis proteins. PARP cleavage is a signature of apoptosis and was detected in 89 kDa. It has been shown in Figure 3.3.3A, PARP cleavage was significantly increased in combination whereas no significant changes were detected in sorafenib and naproxen alone compared to DMSO control in Mahlavu cells.

Caspase-8 and Caspase-9 are proteases that can cleave a variety of proteins in cells. Their expression increases when cells undergo apoptosis. Their expression significantly increased in combination compared to DMSO and Sorafenib. Moreover, Bcl-X proteins are members of the BCL-2 protein family and BCL-X gene has two functionally different products Bcl-xS and Bcl-xL by alternative splicing. (Wimott et al., 2011). Bcl-xL is an anti-apoptotic subunit composed of 233 amino acids detected at 34 kDa whereas Bcl-xS is a pro-apoptotic small subunit consisting of 178 aminoacids detected at nearly 30 kDa. Expression of the small subunit was significantly increased in the combination group compared to DMSO and Sorafenib (Figure 3.3.3A). Figure 3.3.3B shows the increased level of cleaved-PARP and cytochrome-c in Huh7 cells. Overall, it has been shown that apoptosis signaling is enriched upon sorafenib and naproxen combination in HCC.

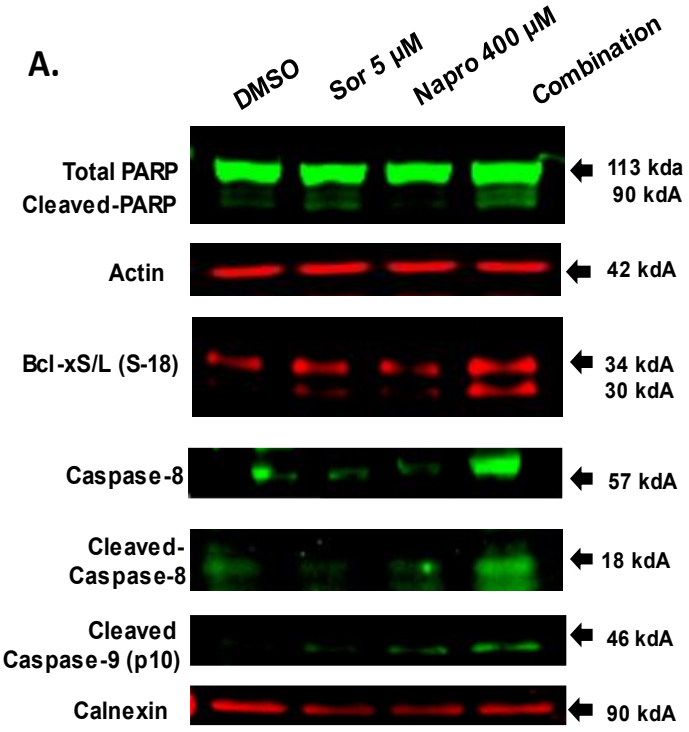

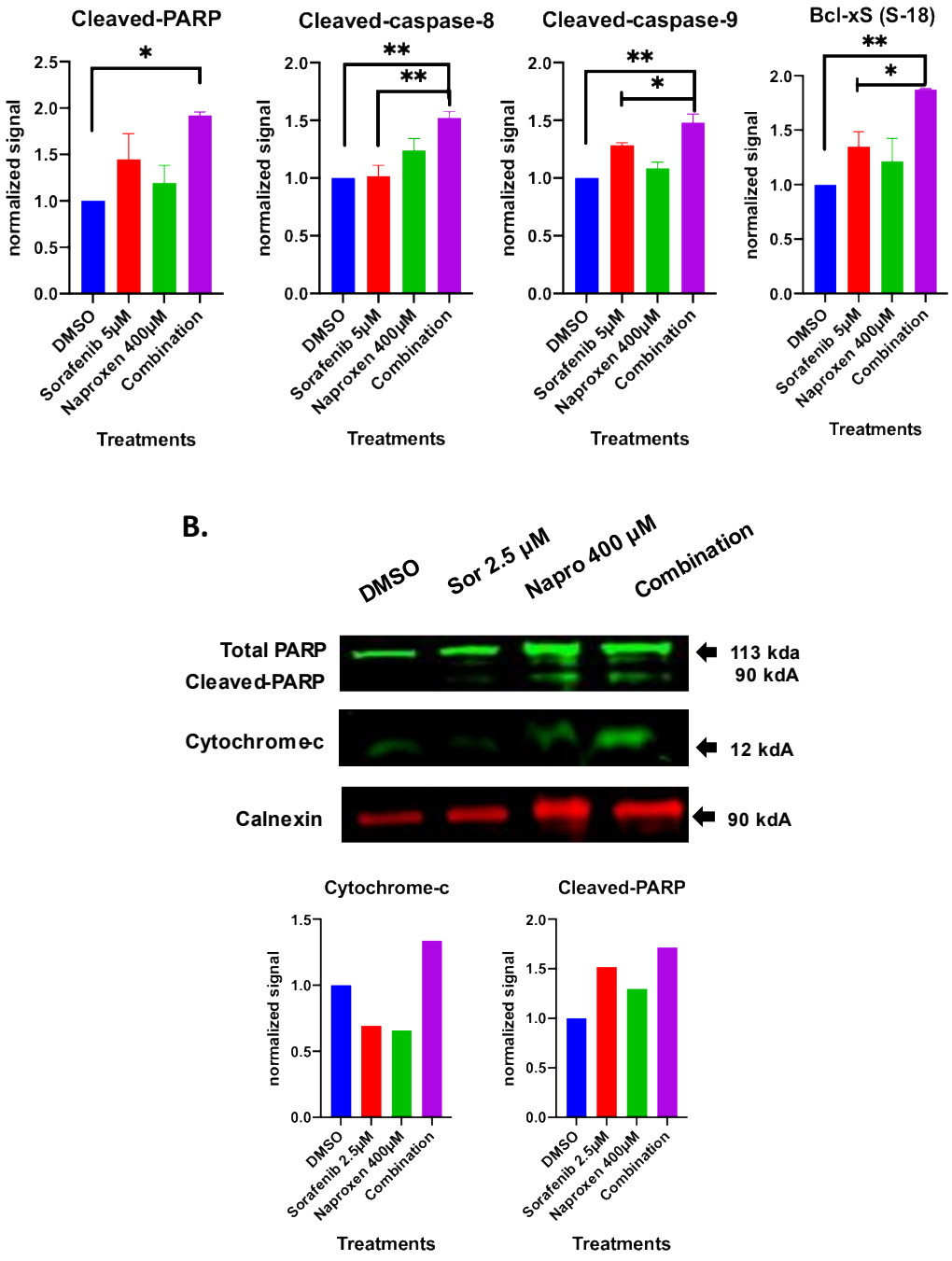

Figure 3.3. 3 Western blot analysis of apoptosis signaling proteins in HCC cell lines. A. Mahlavu cells were treated with the indicated concentration of sorafenib

and Naproxen for 24h. Actin and Calnexin were used as loading controls. Bar graph representation of apoptosis signaling proteins. One-way ANOVA was applied for significance **B.** Huh7 cell treated with the selected concentration of naproxen and sorafenib for 48h. Calnexin was used as the loading control. Bar graphs represent a normalized signal to loading control.

3.4 Combination induces G1 arrest in HCC cell lines

Since we detected apoptosis, we also studied cell cycle arrest in Mahlavu and Huh7 cells. It was shown that the combination induces G1 arrest in HCC cell lines (Figure A.4).

3.5 Investigation of CAPN2 gene in Hepatocellular Carcinoma

As it was shown in figure 3.3.2 CAPN2 found as a common gene from both sorafenib and naproxen network. Therefore, the level of CAPN2 was studied in HCC cell lines. It has been shown that CAPN2 expression is upregulated in a variety of cancer types and mediates tumor invasion and metastasis. Also, Figure 3.5.1 shows that CAPN2 expression is still upregulated even with the treatment of currently used HCC drugs Sorafenib, Regorafenib (Data generated by Dr. Kahraman, (Kahraman et al., 2019), and Lenvatinib (Data generated by Esra Nalbat).

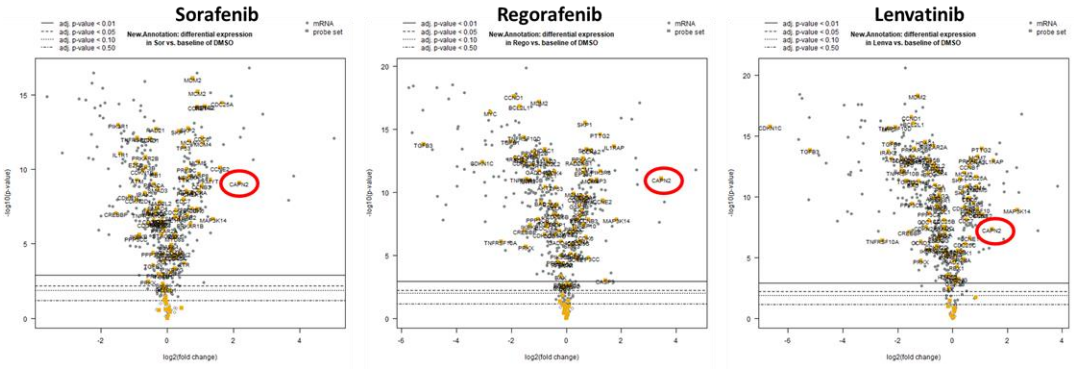

Figure 3.5. 1 CAPN2 expression is upregulated in HCC cell upon treatment with Sorafenib, Regorafenib and Lenvatinib.

Also, It has been demonstrated that a high level of CAPN2 expression corralates with the low rate of survival in all tumor types including HCC (Figure 3.5.2).

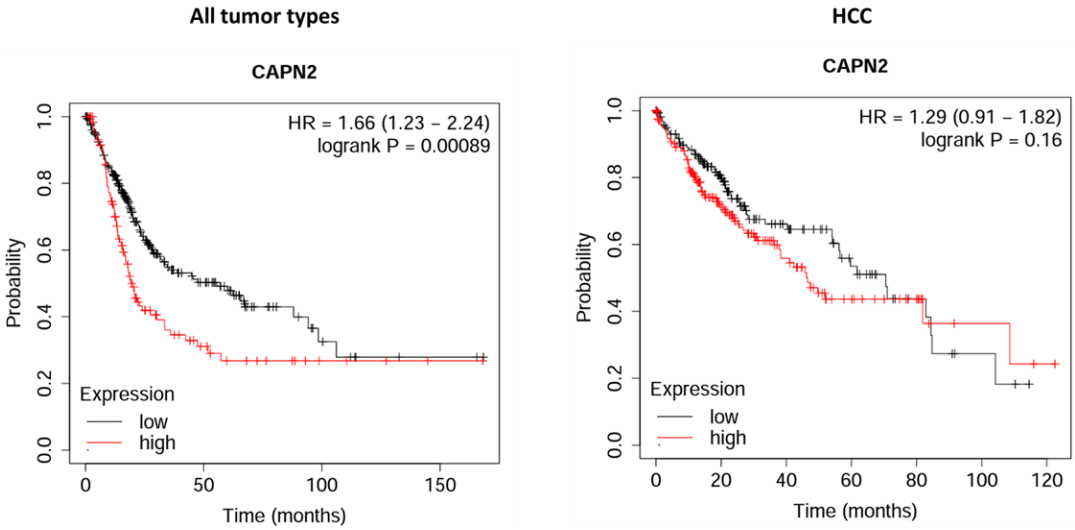

Figure 3.5. 2 Upregulation of CAPN2 associated with low overall survival rate in cancer patients. Kaplan Meier curves were created in https://kmplot.com/ using pan-cancer and liver-cancer mRNA data.

Moreover, our qPCR result (Figure 3.5.3) shows that sorafenib treatment increases CAPN2 expression in both Mahlavu and Huh7 cell lines. However, the combination of the drugs significantly reduced CAPN2 expression, which is up-regulated by sorafenib treatment. Therefore, the unwanted effect of CAPN2 upregulation by

sorafenib treatment can be decreased by sorafenib and naproxen co-treatment. Moreover, since the studies showed that the knockdown of CAPN2 promoted apoptosis in different cancer types, CAPN2 downregulation may be associated with apoptosis in HCC. Therefore, We also hypothesized that CAPN2 down-regulation and apoptosis might be associated with sorafenib and naproxen synergism in HCC.

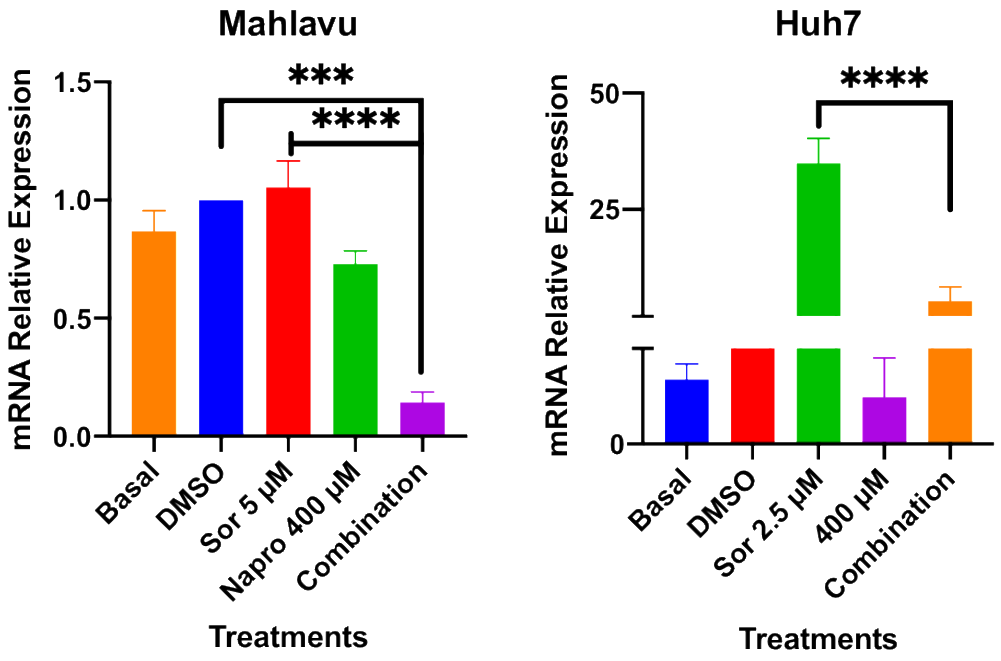

Figure 3.5. 3 CAPN2 relative mRNA expression in HCC cell lines. Mahlavu and Huh7 cells were treated with indicated drugs for 48h. Bar graphs show the relative expression of CAPN2, one-way ANOVA is applied to determine significance.

3.6 Investigation of PI3K pathway activity upon drug combination in HCC cell line

As it is mentioned in section 1.9.1, PI3K/AKT pathway is one of the most commonly deregulated signaling pathways in cancer. Hyperactivity of PI3K/AKT pathway is observed in HCC and its role was well established in acquired drug resistance. It has been known that the down-regulation of PI3K/AKT pathway promotes apoptosis in cells. However, not all cell lines have hyper-active-PI3K/AKT pathway such as Huh7. Expression of PI3K signaling pathway proteins increased in Mahlavu cells but not in Huh7 cells due to PTEN deletion in Mahlavu cell line(Kahraman et al., 2019). Therefore, we studied PI3K/AKT pathway in Mahlavu cells. We found that drug combination significantly reduced AKT pathway mediators at both protein and mRNA levels (Figure 3.6.1).

A.

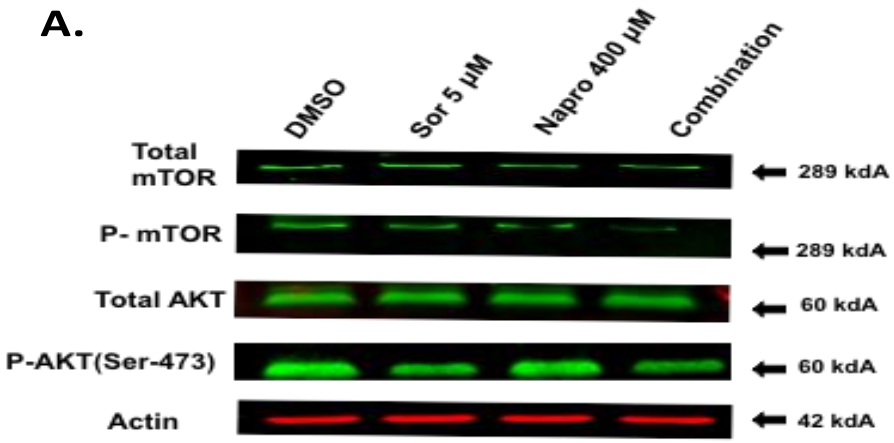
DMSO
Sor 5 µM
Napro 400 µM
Combination
Total mTOR
289 kdA
P- mTOR
289 kdA
Total AKT
60 kdA
P-AKT(Ser-473)
60 kdA
Actin
42 kdA

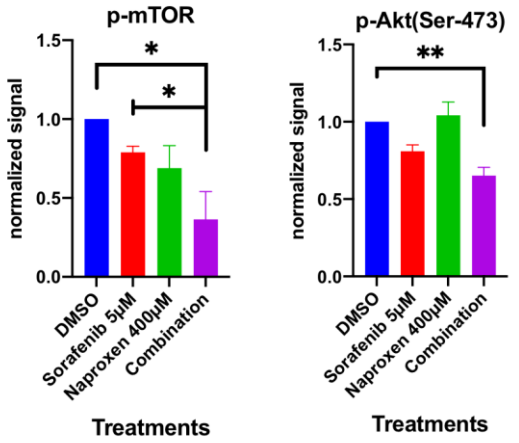
p-mTOR
normalized signal
1.5
1.0
0.5
0.0
*
*
DMSO
Sorafenib 5µM
Naproxen 400µM
Combination
Treatments
p-Akt(Ser-473)
normalized signal
1.5
1.0
0.5
0.0
**
DMSO
Sorafenib 5µM
Naproxen 400µM
Combination
Treatments

B.

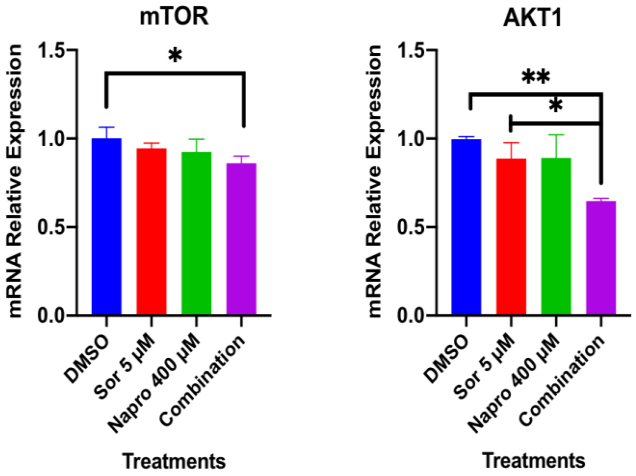
mTOR
mRNA Relative Expression
1.5
1.0
0.5
0.0
*
DMSO
Sor 5 µM
Napro 400 µM
Combination
Treatments
AKT1
mRNA Relative Expression
1.5
1.0
0.5
0.0
**
*
DMSO
Sor 5 µM
Napro 400 µM
Combination
Treatments

Figure 3.6. 1 Drug combination decreases the activity of PI3K/AKT pathway. **A**. Western blot analysis of PI3K/AKT pathway proteins. Bar graphs represent the changes in the level of p-mTOR and p-AKT proteins in 24h. **B.** Bar graphs represent changes in mRNA level of AKT and mTOR genes in 24h. One-way ANOVA was applied for significance.

CHAPTER 4

CONCLUSION AND DISCUSSION

This study shows that, for the first time, FDA-approved sorafenib and naproxen have synergistic interaction on hepatocellular carcinoma. Our initial aim was to find a synergistic interaction between FDA-approved non-steroidal anti-inflammatory drugs (NSAIDs) and HCC drugs. Among different NSAIDs and HCC drugs, Naproxen and Sorafenib combination was selected as the most synergistic one according to the synergy score, calculated by either the *synergyfinder* tool or R programming. Apart from the synergy score, Synergyfinder tool and R also gives us the most synergistic area. Based on this information, 5 μM and 2.5 μM of sorafenib were selected for Mahlavu and Huh7 cell lines, respectively. On the other hand, 400 μM naproxen was selected for both cell lines. In the line of NSAIDs study in cancer, a higher concentration of NSAIDs was used (2000 μM or 4000 μM) (Kim et al., 2014), (Xia et al., 2017). Compared to the literature, we showed synergy in lower concentrations.

Mahlavu is one of the most aggressive HCC cell lines, which has PTEN deletion and hyperactive AKT signaling. It is a mesenchymal cell line that can metastasize and migrate, whereas Huh7 is an epithelial-like cell, one of the most common cell types used in HCC studies. Moreover, IC_{50} of sorafenib was approximately 5 μM for Mahlavu and 2.5 μM for Huh7. Therefore, the selected doses for the study were reasonable, considering the differences between the two cell lines.

To elucidate the signaling pathways that may propagate synergism, transcriptomic data sets of sorafenib and naproxen in HCC cell lines were utilized to perform network reconstruction analysis. This enabled the identification of the hidden targets of the drugs besides their immediate target and signaling pathways modulated within this interaction.

CMAP database is a comprehensive database including over 1 million gene expression signatures from different cell types. Naproxen-treated Huh7 gene expression data was utilized from this database to construct naproxen network in the Huh7 cell line. On the other hand, Sorafenib-treated Huh7 RNA sequencing data was gathered from OMICSDI-EMTAB-7847. Although the experimental conditions differed for naproxen, (15 μM Naproxen for 72h of treatment), 400 μM naproxen also did not significantly affect cell proliferation and apoptosis induction. Moreover, the Anti-cancer activity of various NSAIDs, including naproxen, is observable only when the drugs are used in high concentration. Therefore, the network constructed with 15 μM of naproxen-treated Huh7 data also gave us information to a certain level. Moreover, network analysis revealed that naproxen and sorafenib networks are topologically separated, which indicates that they modulate different signaling cascades in cells. Drugs that are known to have experimentally synergistic interactions were utilized to perform network analysis which resulted in topologically separated networks (Unsal-Beyge & Tuncbag, 2022) This is the case that we observed in our network analysis.

Overall, network data showed that apoptosis pathways were enriched in both sorafenib and naproxen networks. Therefore, we studied apoptosis signaling in Huh7 and Mahlavu cells treated with selected concentrations of naproxen and sorafenib by performing Annexin-V/PI staining, Hoechst staining, and western blot analysis. Apoptosis was examined for different time points (24h, 48h, and 72h). Hoechst staining indicated that apoptotic nuclear structures start to form after 24h, and become more apparent in 48h and 72h. Annexin-V/PI staining quantified an increase in apoptotic cell population after 72h. Finally, western blot was performed to examine the proteins that mediate apoptosis signaling. It was shown that levels of pro-apoptotic proteins such as cleaved caspase-8 and caspase-9, cleaved-PARP, Bcl-xS and cytochrome-c were significantly increased in the combination group and indicated that naproxen and sorafenib combination promotes apoptosis in HCC cell lines.

Moreover, gene networks were studied by focusing on the CAPN2 gene, which was found to be the only gene mediated by both sorafenib and naproxen network. It has been shown that CAPN2 up-regulation is not only associated with proliferation and metastasis in cancer (Miao et al., 2017), (Peng., 2022), but also associated with decreased survival rate in cancer patients, including HCC.

Our findings show that the CAPN2 was upregulated by sorafenib and down-regulated by naproxen; the combination of the drugs significantly reduces CAPN2 expression which is upregulated by sorafenib treatment. This is valuable because CAPN2 up-regulation is undesirable since it increases metastasis, invasion and proliferation and is associated with a low survival rate in HCC. According to qPCR result; CAPN2 expression is lower in the Huh7 cells which is also supported by the harmonizome database. (Rouillard et al., 2016). The basal level of CAPN2 expression is higher in Mahlavu which is one of the most aggressive cell types of HCC. Moreover, the pattern for each cell line possesses a similar outcome, where sorafenib increases and naproxen decreases CAPN2 expression, yet co-treatment of the drugs significantly decreases CAPN2 expression.

Moreover, CAPN2 silencing promotes apoptosis in HCC (G. Zhang et al., 2018). Thus, we hypothesized that CAPN2 down-regulation may be associated with apoptosis induction that we observed in HCC cell lines.

Moreover, the PI3K-AKT pathway is the most commonly deregulated signaling pathway in HCC, and its deregulation posses an uncontrolled proliferation signal. Once it is deregulated, the cell can escape from apoptosis and induce proliferation. On the contrary, once its activity is suppressed, the cell undergoes apoptosis. We show that the activity of PI3K-AKT signaling is decreased in combination compared to sorafenib and naproxen alone in Mahlavu cell line. Moreover, it has been shown in many studies that CAPN2 down-regulation is associated with decreased activity of AKT pathway. Our results also pointed out that apoptosis induction may be further associated with the down-regulation of the CAPN2 gene and the decreasing activity of the PI3K-AKT pathway in HCC as it was illustrated in Figure 4.1.

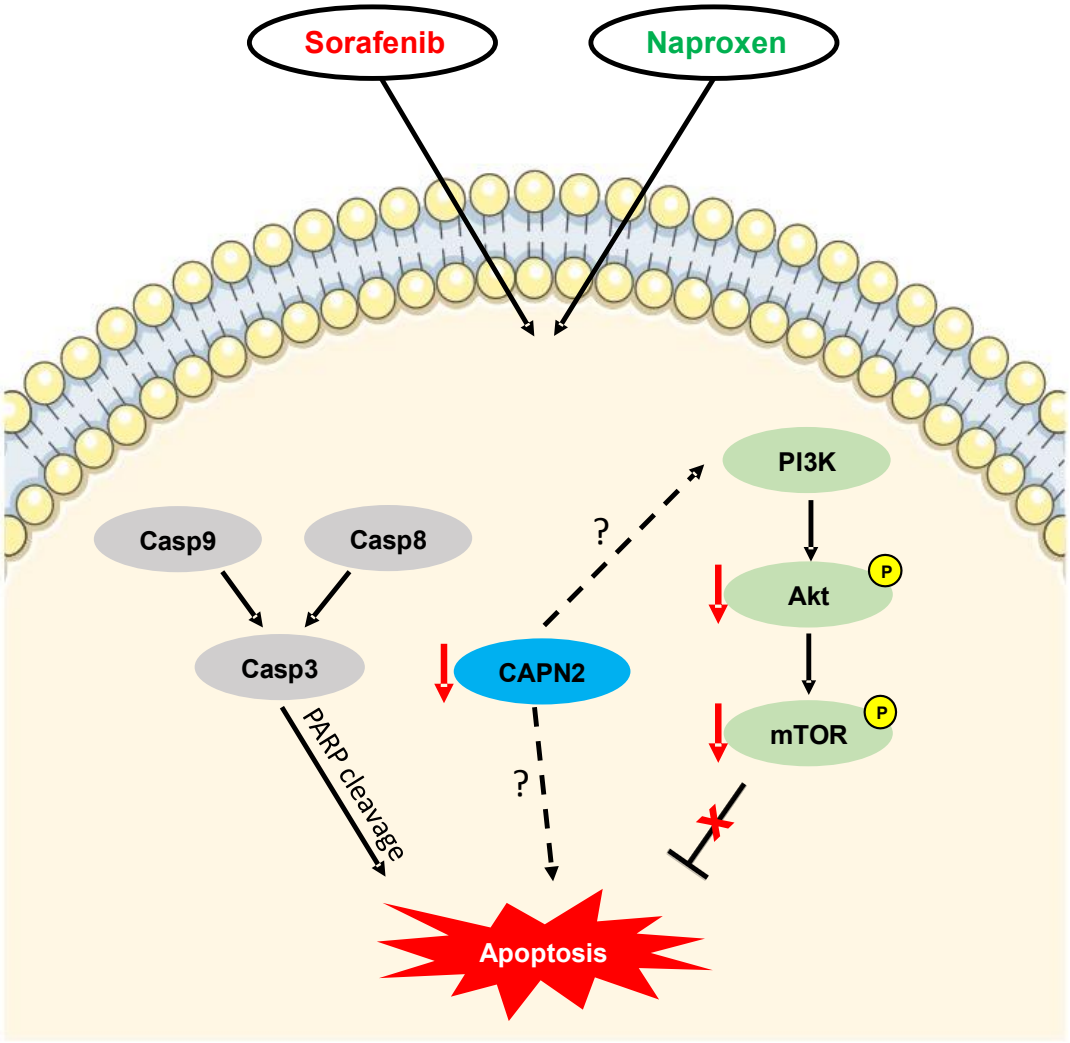

Figure 4. 1 Summary of this study. Sorafenib and Naproxen combination induces apoptosis in HCC. The activity of AKT signaling and CAPN2 expression decreased upon drug combination.

CHAPTER 5

FUTURE PERSPECTIVES

In this study, the mechanism behind synergistic interaction of sorafenib and naproxen combination was investigated, and it has been found that synergistic interaction is mediated by increasing apoptosis in HCC cell lines. This combination was proposed for the first time as a novel drug combination for HCC.

Moreover, for the future perspective of this study, several questions need to be addressed.

1-Since our transcriptomic analysis was performed using data from Huh7 cells treated with sorafenib alone or naproxen alone, the transcriptomic analysis could also be performed for sorafenib and naproxen co-treatment and integrated into the established network to improve the outcome of the network-based analysis.

2-Since our study pointed out that apoptosis induction in HCC lines could be associated with the down-regulation of CAPN2 and decreasing the activity of PI3K/AKT/mTOR signaling, this association could be further investigated. For the relationship of CAPN2, apoptosis, and AKT pathway signaling, several knock-out and knock-in experiments should be performed. CAPN2 gene can be overexpressed, then apoptosis and AKT signaling can be studied by western blot. Moreover, PTEN can be overexpressed in Mahlavu cell line to reduce the activity of AKT signaling. Subsequently, apoptosis signaling and changes in the level of CAPN2 expression can be studied.

3- It has been known from both clinical and experimental data; sorafenib eventually causes drug resistance. Therefore, Naproxen and sorafenib combination could be studied in terms of targeting sorafenib resistance. Also, It has been shown that the combination of sorafenib with NSAIDs decreases the stem cell population compared to sorafenib alone. (Kahraman et al., 2022). Stemness is also an important aspect of

resistance. Therefore, the effect of the naproxen and sorafenib combination on stemness could be further studied.

REFERENCES

Aytaç, P. S., Durmaz, I., Houston, D. R., Çetin-Atalay, R., & Tozkoparan, B. (2016). Novel triazolothiadiazines act as potent anticancer agents in liver cancer cells through Akt and ASK-1 proteins. *Bioorganic and Medicinal Chemistry*, *24*(4), 858-872. https://doi.org/10.1016/j.bmc.2016.01.013

Bishayee, A. (2014). The role of inflammation in liver cancer. *Advances in Experimental Medicine and Biology*, *816*, 401-435. https://doi.org/10.1007/978-3-0348-0837-8_16

Brutzkus, N. J. (n.d.). *Continuing Education Activity*. https://www.ncbi.nlm.nih.gov/books/NBK525965/#_NBK525965_pubdet_

Budhu, A., & Wang, X. W. (2006). The role of cytokines in hepatocellular carcinoma. *Journal of Leukocyte Biology*, *80*(6), 1197–1213. https://doi.org/10.1189/jlb.0506297

Buontempo, F., Ersahin, T., Missiroli, S., Senturk, S., Etro, D., Ozturk, M., Capitani, S., Cetin-Atalay, R., & Neri, M. L. (2011). Inhibition of Akt signaling in hepatoma cells induces apoptotic cell death independent of Akt activation status. *Investigational New Drugs*, *29*(6), 1303-1313. https://doi.org/10.1007/s10637-010-9486-3

Carneiro, B. A., & El-Deiry, W. S. (2020). Targeting apoptosis in cancer therapy. In *Nature Reviews Clinical Oncology*, *17(*7), 395–417. https://doi.org/10.1038/s41571-020-0341-y

Chang, F., Lee, J. T., Navolanic, P. M., Steelman, L. S., Shelton, J. G., Blalock, W. L., Franklin, R. A., & McCubrey, J. A. (2003). Involvement of PI3K/Akt pathway in cell cycle progression, apoptosis, and neoplastic transformation: A target for cancer chemotherapy. In *Leukemia*, *17*(3), 590-603. https://doi.org/10.1038/sj.leu.2402824

Chen, S. C., Huang, Y. H., Chen, M. H., Hung, Y. P., Lee, R. C., Shao, Y. Y., & Chao, Y. (2022). Anti-PD-1 combined sorafenib versus anti-PD-1 alone in the treatment of advanced hepatocellular cell carcinoma: a propensity score-matching study. *BMC Cancer*, *22*(1), 55. https://doi.org/10.1186/s12885-022-09173-4

Cheng, F., Desai, R. J., Handy, D. E., Wang, R., Schneeweiss, S., Barabási, A. L., & Loscalzo, J. (2018). Network-based approach to prediction and population-based validation of in silico drug repurposing. *Nature Communications*, *9*(1), 2691. https://doi.org/10.1038/s41467-018-05116-5

Deng, S., Solinas, A., & Calvisi, D. F. (2021). Cabozantinib for HCC Treatment, From Clinical Back to Experimental Models. In *Frontiers in Oncology*, *11, 756672*. https://doi.org/10.3389/fonc.2021.756672

Duarte, D., & Vale, N. (2022). Evaluation of synergism in drug combinations and reference models for future orientations in oncology. In *Current Research in Pharmacology and Drug Discovery, 3,* 100110. https://doi.org/10.1016/j.crphar.2022.100110

Elmore, S. (2007). Apoptosis: A Review of Programmed Cell Death. In *Toxicologic Pathology*, *35*(4), 495-516. https://doi.org/10.1080/01926230701320337

Greenspan, E. J., Madigan, J. P., Boardman, L. A., & Rosenberg, D. W. (2011). Ibuprofen inhibits activation of nuclear β-catenin in human colon adenomas and induces the phosphorylation of GSK-3β. *Cancer Prevention Research*, *4*(1), 161-171. https://doi.org/10.1158/1940-6207.CAPR-10-0021

Guney, E., Menche, J., Vidal, M., & Barábasi, A. L. (2016). Network-based in silico drug efficacy screening. *Nature Communications*, *7,* 1-13. https://doi.org/10.1038/ncomms10331

Hanada, M., Feng, J., & Hemmings, B. A. (2004). Structure, regulation and function of PKB/AKT - A major therapeutic target. *Biochimica et*

Biophysica Acta - Proteins and Proteomics, *1697*(1–2), 3-16. https://doi.org/10.1016/j.bbapap.2003.11.009

Hayato, N., & Shin, M. (2012). Inflammation- and stress-related signaling pathways in hepatocarcinogenesis. *World Journal of Gastroenterology 18*(31), 4071. https://doi.org/10.3748/wjg.v18.i31.4071

Hsu, M. H., Hsu, S. M., Kuo, Y. C., Liu, C. Y., Hsieh, C. Y., Twu, Y. C., Wang, C. K., Wang, Y. H., & Liao, Y. J. (2017). Treatment with low-dose sorafenib in combination with a novel benzimidazole derivative bearing a pyrolidine side chain provides synergistic anti-proliferative effects against human liver cancer. *RSC Advances*, *7*(26), 16253-16263. https://doi.org/10.1039/c6ra28281d

Jia, J., Zhu, F., Ma, X., Cao, Z. W., Li, Y. X., & Chen, Y. Z. (2009). Mechanisms of drug combinations: Interaction and network perspectives. *Nature Reviews Drug Discovery*, *8*(2), 111-128. https://doi.org/10.1038/nrd2683

Kahraman, D. C., Bilget Guven, E., Aytac, P. S., Aykut, G., Tozkoparan, B., & Cetin Atalay, R. (2022). A new triazolothiadiazine derivative inhibits stemness and induces cell death in HCC by oxidative stress dependent JNK pathway activation. *Scientific Reports*, *12*(1), 15139. https://doi.org/10.1038/s41598-022-17444-0

Kahraman, D. C., Kahraman, T., & Cetin-Atalay, R. (2019). Targeting PI3K/AKT/mTOR pathway identifies differential expression and functional role of IL8 in liver cancer stem cell enrichment. *Molecular Cancer Therapeutics*, *18*(11), 2146-2157. https://doi.org/10.1158/1535-7163.MCT-19-0004

Kelderman, S., Schumacher, T. N. M., & Haanen, J. B. A. G. (2014). Acquired and intrinsic resistance in cancer immunotherapy. In *Molecular Oncology 8(*6), 1132-1139. https://doi.org/10.1016/j.molonc.2014.07.011

Kim, M. S., Kim, J. E., Lim, D. Y., Huang, Z., Chen, H., Langfald, A., Lubet, R. A., Grubbs, C. J., Dong, Z., & Bode, A. M. (2014). Naproxen induces

cell-cycle arrest and apoptosis in human urinary bladder cancer cell lines and chemically induced cancers by targeting PI3K. *Cancer Prevention Research*, *7*(2), 236-245. https://doi.org/10.1158/1940-6207.CAPR-13-0288

Kroemer, G., Galluzzi, L., & Brenner, C. (2007). *Mitochondrial Membrane Permeabilization in Cell Death*, *87*(1), 99-163. https://doi.org/10.1152/physrev.00013.2006.-Irrespective

LaCasse, E. C., Mahoney, D. J., Cheung, H. H., Plenchette, S., Baird, S., & Korneluk, R. G. (2008). IAP-targeted therapies for cancer. In *Oncogene*, *27*(48), 6252-6275. https://doi.org/10.1038/onc.2008.302

Lei, M., Ma, G., Sha, S., Wang, X., Feng, H., Zhu, Y., & Du, X. (2019). Dual-functionalized liposome by co-delivery of paclitaxel with sorafenib for synergistic antitumor efficacy and reversion of multidrug resistance. *Drug Delivery*, *26*(1), 262-272. https://doi.org/10.1080/10717544.2019.1580797

Lippert, T. H., Ruoff, H. J., & Volm, M. (2008). Intrinsic and acquired drug resistance in malignant tumors: The main reason for therapeutic failure. In *Arzneimittel-Forschung/Drug Research*, *58*(06), 261-264. https://doi.org/10.1055/s-0031-1296504

Llovet, J. M., Kelley, R. K., Villanueva, A., Singal, A. G., Pikarsky, E., Roayaie, S., Lencioni, R., Koike, K., Zucman-Rossi, J., & Finn, R. S. (2021). Hepatocellular carcinoma. In *Nature Reviews Disease Primers*, *7(*1). https://doi.org/10.1038/s41572-020-00240-3

Llovet, J. M., Ricci, S., Mazzaferro, V., Hilgard, P., Gane, E., Blanc, J.-F., de Oliveira, A. C., Santoro, A., Raoul, J.-L., Forner, A., Schwartz, M., Porta, C., Zeuzem, S., Bolondi, L., Greten, T. F., Galle, P. R., Seitz, J.-F., Borbath, I., Häussinger, D., Bruix, J. (2008). Sorafenib in Advanced Hepatocellular Carcinoma. *New England Journal of Medicine*, *359*(4), 378-390. https://doi.org/10.1056/nejmoa0708857

Ma, X. L., Zhu, K. Y., Chen, Y. da, Tang, W. G., Xie, S. H., Zheng, H., Tong, Y., Wang, Y. C., Ren, N., Guo, L., & Lu, R. Q. (2022). Identification of a novel Calpain-2-SRC feed-back loop as necessity for β-Catenin accumulation and signaling activation in hepatocellular carcinoma. *Oncogene*, *41*(27), 3554–3569. https://doi.org/10.1038/s41388-022-02367-x

Markiewski, M. M., DeAngelis, R. A., & Lambris, J. D. (2006). Liver inflammation and regeneration: Two distinct biological phenomena or parallel pathophysiologic processes? In *Molecular Immunology*, 43(1-2), 45–56. https://doi.org/10.1016/j.molimm.2005.06.019

Menche, J., Sharma, A., Kitsak, M., Ghiassian, S. D., Vidal, M., Loscalzo, J., & Barabási, A. L. (2015). Uncovering disease-disease relationships through the incomplete interactome. *Science*, *347*(6224), 1257601. https://doi.org/10.1126/science.1257601

Miao, C., Liang, C., Tian, Y., Xu, A., Zhu, J., Zhao, K., Zhang, J., Hua, Y., Liu, S., Dong, H., Zhang, C., Su, S., Li, P., Qin, C., & Wang, Z. (2017). Overexpression of CAPN2 promotes cell metastasis and proliferation via AKT/mTOR signaling in renal cell carcinoma. *Oncotarget*, *8*(58), 97811. https://doi.org/10.18632/oncotarget.22083

Mokhtari, R. B., Homayouni, T. S., Baluch, N., Morgatskaya, E., Kumar, S., Das, B., & Yeger, H. (2017). Combination therapy in combating cancer. In *Oncotarget*, *8*(23), 38022-38043. https://doi.org/10.18632/oncotarget.16723

Morisaki, T., Umebayashi, M., Kiyota, A., Koya, N., Tanaka, H., Onishi, H., & Katano, M. (2013). Combining celecoxib with sorafenib synergistically inhibits hepatocellular carcinoma cells In Vitro. *Anticancer Research*, *33*(4), 1387-1395.

Motawi, T. M. K., Bustanji, Y., El-Maraghy, S., Taha, M. O., & Al-Ghussein, M. A. S. (2014). Evaluation of naproxen and cromolyn activities against cancer cells viability, proliferation, apoptosis, p53 and gene expression of

survivin and caspase-3. *Journal of Enzyme Inhibition and Medicinal Chemistry*, *29*(2), 153-161. https://doi.org/10.3109/14756366.2012.762645

Omar, H. A., Tolba, M. F., Hung, J. H., & Al-Tel, T. H. (2016). OSU-2S/Sorafenib synergistic antitumor combination against hepatocellular carcinoma: The role of PKCd/p53. *Frontiers in Pharmacology*, *7*, 463. https://doi.org/10.3389/fphar.2016.00463

Ozturk, N., Erdal, E., Mumcuoglu, M., Akcali, K. C., Yalcin, O., Senturk, S., Arslan-Ergul, A., Gur, B., Yulug, I., Cetin-Atalay, R., Yakicier, C., Yagci, T., Tez, M., & Ozturk, M. (2006). Reprogramming of replicative senescence in hepatocellular carcinoma-derived cells. *Proceedings of the National Academy of Sciences of the United States of America*, *103*(7), 2178-2183. https://doi.org/10.1073/pnas.0510877103

Pang, Q., Jin, H., Qu, K., Man, Z., Wang, Y., Yang, S., Zhou, L., & Liu, H. (2017). The effects of nonsteroidal anti-inflammatory drugs in the incident and recurrent risk of hepatocellular carcinoma: A meta-analysis. *OncoTargets and Therapy*, *10*, 4645. https://doi.org/10.2147/OTT.S143154

Peng, X., Yang, R., Song, J., Wang, X., & Dong, W. (2022). Calpain2 Upregulation Regulates EMT-Mediated Pancreatic Cancer Metastasis via the Wnt/β-Catenin Signaling Pathway. *Frontiers in Medicine*, *9*, 1413. https://doi.org/10.3389/fmed.2022.783592

Pfeffer, C. M., & Singh, A. T. K. (2018). Apoptosis: A target for anticancer therapy. *International Journal of Molecular Sciences*, *19*(2), 448. https://doi.org/10.3390/ijms19020448

Rausch, V., Liu, L., Kallifatidis, G., Baumann, B., Mattern, J., Gladkich, J., Wirth, T., Schemmer, P., Büchler, M. W., Zöller, M., Salnikov, A. v., & Herr, I. (2010). Synergistic activity of sorafenib and sulforaphane abolishes pancreatic cancer stem cell characteristics. *Cancer Research*, *70*(12), 5004-5013. https://doi.org/10.1158/0008-5472.CAN-10-0066

Rayburn, E. R., Ezell, S. J., & Zhang, R. (2009). Anti-inflammatory agents for cancer therapy. *Molecular and Cellular Pharmacology*, *1*(1), 29. https://doi.org/10.4255/mcpharmacol.09.05

Reed, J. C., Jurgensmeier, J. M., & Matsuyama, S. (n.d.). *Bcl-2 family proteins and mitochondria*.

Refolo, M. G., Messa, C., Guerra, V., Carr, B. I., & D'alessandro, R. (2020). Inflammatory mechanisms of hcc development. In *Cancers*, *12*(3), 641. https:// doi.org/10.3390/cancers1203064194/12/3/641

Roell, K. R., Reif, D. M., & Motsinger-Reif, A. A. (2017). An introduction to terminology and methodology of chemical synergy-perspectives from across disciplines. In *Frontiers in Pharmacology*, *8*, 158. https://doi.org/10.3389/fphar.2017.00158

Rouillard, A. D., Gundersen, G. W., Fernandez, N. F., Wang, Z., Monteiro, C. D., McDermott, M. G., & Ma'ayan, A. (2016). The harmonizome: a collection of processed datasets gathered to serve and mine knowledge about genes and proteins. *Database : The Journal of Biological Databases and Curation*, *2016*. https://doi.org/10.1093/database/baw100

Roviello, G., Sohbani, N., Petrioli, R., & Rodriquenz, M. G. (2019). Ramucirumab as a second line therapy for advanced HCC: a significant achievement or a wasted opportunity for personalised therapy? In *Investigational New Drugs*, 37(6), 1274-1288. https://doi.org/10.1007/s10637-019-00760-0

Sahasrabuddhe, V. v., Gunja, M. Z., Graubard, B. I., Trabert, B., Schwartz, L. M., Park, Y., Hollenbeck, A. R., Freedman, N. D., & Mcglynn, K. A. (2012). Nonsteroidal anti-inflammatory drug use, chronic liver disease, and hepatocellular carcinoma. *Journal of the National Cancer Institute*, *104*(23), 1808-1814. https://doi.org/10.1093/jnci/djs452

Sanduzzi-Zamparelli, M., Díaz-Gonzalez, Á., & Reig, M. (2019). New Systemic Treatments in Advanced Hepatocellular Carcinoma. In *Liver Transplantation*, *25*(2), 311-322. https://doi.org/10.1002/lt.25354

Tai, W. T., Chu, P. Y., Shiau, C. W., Chen, Y. L., Li, Y. S., Hung, M. H., Chen, L. J., Chen, P. L., Su, J. C., Lin, P. Y., Yu, H. C., & Chen, K. F. (2014). STAT3 mediates regorafenib-induced apoptosis in hepatocellular carcinoma. *Clinical Cancer Research*, *20*(22). https://doi.org/10.1158/1078-0432.CCR-14-0725

Tuncbag, N., Gosline, S. J. C., Kedaigle, A., Soltis, A. R., Gitter, A., & Fraenkel, E. (2016). Network-Based Interpretation of Diverse High-Throughput Datasets through the Omics Integrator Software Package. *PLoS Computational Biology*, *12*(4), e1004879. https://doi.org/10.1371/journal.pcbi.1004879

Unsal-Beyge, S., & Tuncbag, N. (2022). Functional stratification of cancer drugs through integrated network similarity. *Npj Systems Biology and Applications*, *8*(1), 11. https://doi.org/10.1038/s41540-022-00219-8

Wang, X., Zhang, H., & Chen, X. (2019). Drug resistance and combating drug resistance in cancer. In *Cancer Drug Resistance*, *2*(2), 141-160. https://doi.org/10.20517/cdr.2019.10

Wehling, M. (2014). Non-steroidal anti-inflammatory drug use in chronic pain conditions with special emphasis on the elderly and patients with relevant comorbidities: Management and mitigation of risks and adverse effects. In *European Journal of Clinical Pharmacology, 70*(10), 1159-1172. https://doi.org/10.1007/s00228-014-1734-6

Wong, R. S. Y. (2011). Apoptosis in cancer: From pathogenesis to treatment. In *Journal of Experimental and Clinical Cancer Research, 30*(1), 1-14. https://doi.org/10.1186/1756-9966-30-87

Xia, H., Lee, K. W., Chen, J., Kong, S. N., Sekar, K., Deivasigamani, A., Seshachalam, V. P., Goh, B. K. P., Ooi, L. L., & Hui, K. M. (2017). Simultaneous silencing of ACSL4 and induction of GADD45B in hepatocellular carcinoma cells amplifies the synergistic therapeutic effect of aspirin and sorafenib. *Cell Death Discovery*, *3*(1), 1-10. https://doi.org/10.1038/cddiscovery.2017.58

Yang, J. D., Hainaut, P., Gores, G. J., Amadou, A., Plymoth, A., & Roberts, L. R. (2019). A global view of hepatocellular carcinoma: trends, risk, prevention and management. In *Nature Reviews Gastroenterology and Hepatology*, *16*(10), 589–604. https://doi.org/10.1038/s41575-019-0186-y

Yang, J., Yan, L., & Wang, W. (2012). Current status of multimodal & combination therapy for hepatocellular carcinoma. In *Indian Journal of Medical Research 136*(3), 391-403.

Yao, X., Zhao, C. ru, Yin, H., Wang, K. W., & Gao, J. jun. (2020). Synergistic antitumor activity of sorafenib and artesunate in hepatocellular carcinoma cells. *Acta Pharmacologica Sinica*, *41*(12), 1609-1620. https://doi.org/10.1038/s41401-020-0395-5

Yu, L. X., Ling, Y., & Wang, H. Y. (2018). Role of nonresolving inflammation in hepatocellular carcinoma development and progression. In *npj Precision Oncology*, *2*(1), 6. https://doi.org/10.1038/s41698-018-0048-z

Zhang, G., Fang, T., Chang, M., Li, J., Hong, Q., Bai, C., & Zhou, J. (2018). Calpain 2 knockdown promotes cell apoptosis and restores gefitinib sensitivity through epidermal growth factor receptor/protein kinase B/survivin signaling. *Oncology Reports*, *40*(4), 1937–1946. https://doi.org/10.3892/or.2018.6625

Zhang, H., Zhang, W., Jiang, L., & Chen, Y. (2022). Recent advances in systemic therapy for hepatocellular carcinoma. In *Biomarker Research*, *10*(1), 1-21. https://doi.org/10.1186/s40364-021-00350-4

APPENDICES

A. SUPPLEMENTARY FIGURES

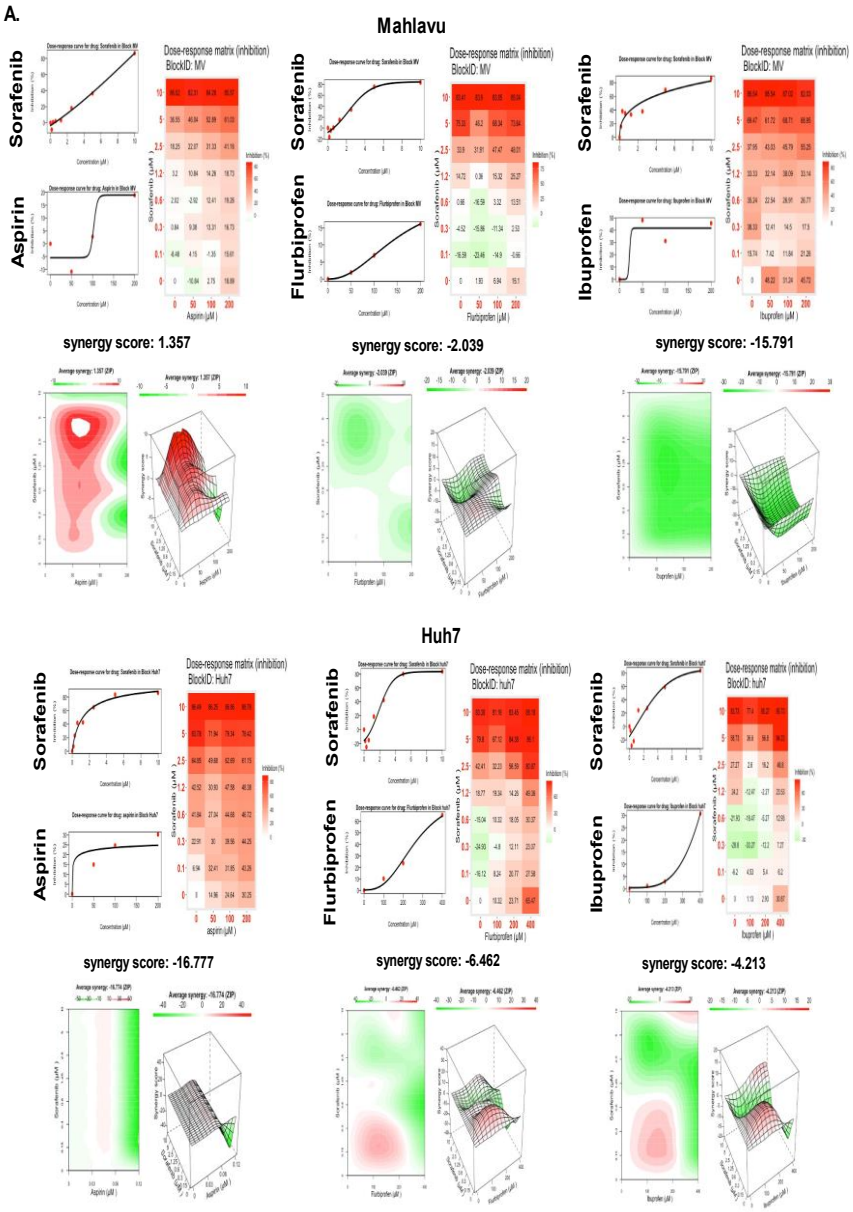

B.

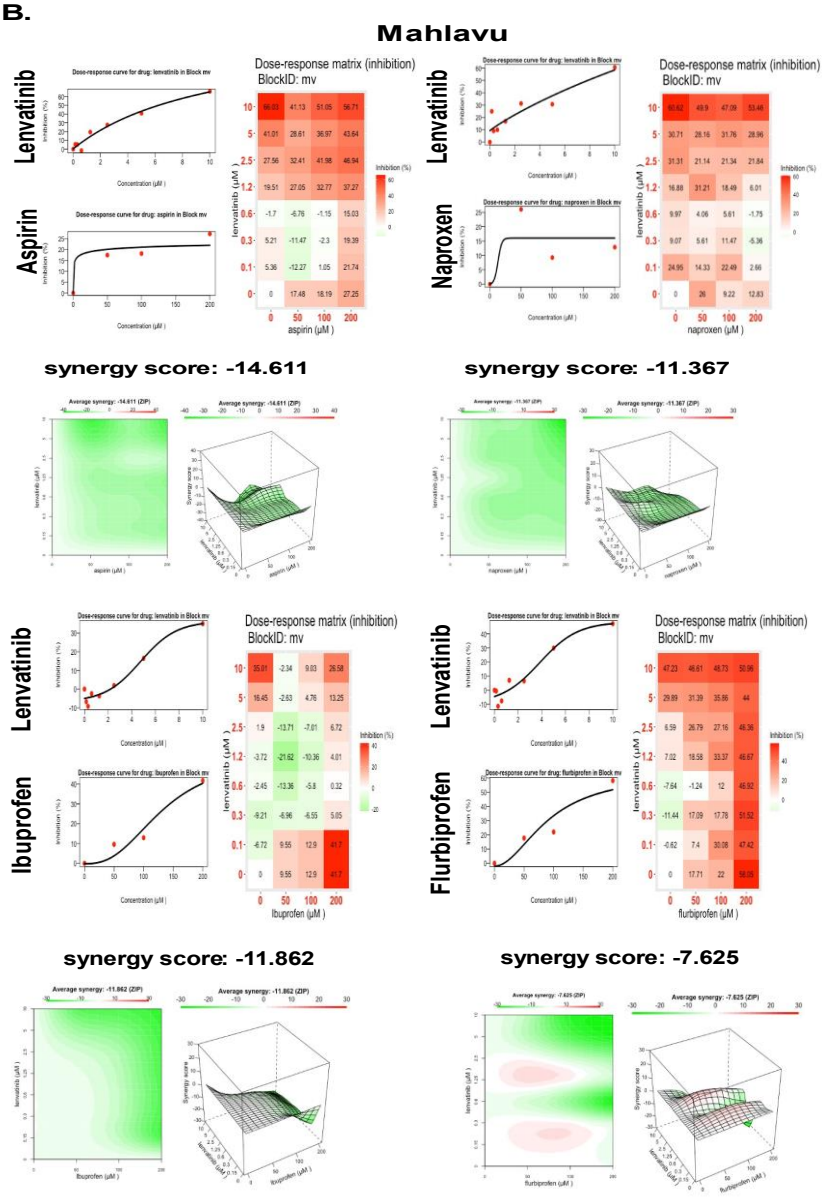
Mahlavu
Lenvatinib
Aspirin
Dose-response matrix (inhibition)
BlockID: mv
lenvatinib (μM)
aspirin (μM)
synergy score: -14.611
Lenvatinib
Naproxen
Dose-response matrix (inhibition)
BlockID: mv
lenvatinib (μM)
naproxen (μM)
synergy score: -11.367
Lenvatinib
Ibuprofen
Dose-response matrix (inhibition)
BlockID: mv
lenvatinib (μM)
Ibuprofen (μM)
synergy score: -11.862
Lenvatinib
Flurbiprofen
Dose-response matrix (inhibition)
BlockID: mv
lenvatinib (μM)
flurbiprofen (μM)
synergy score: -7.625

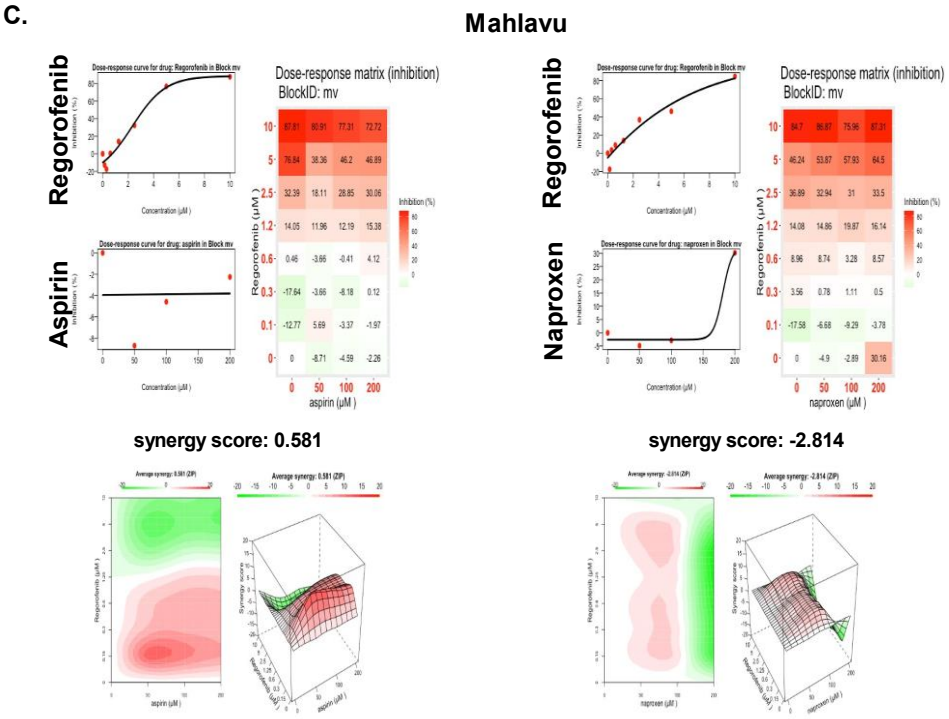

Figure A.1 Effect of other combinations in HCC cell lines. Dose-response matrix and synergy score for **A.** Sorafenib combination **B.** Lenvatinib combination with indicated drugs in Mahlavu cell lines. **C.** Regorofenib combination with aspirin and naproxen on Mahlavu cell.

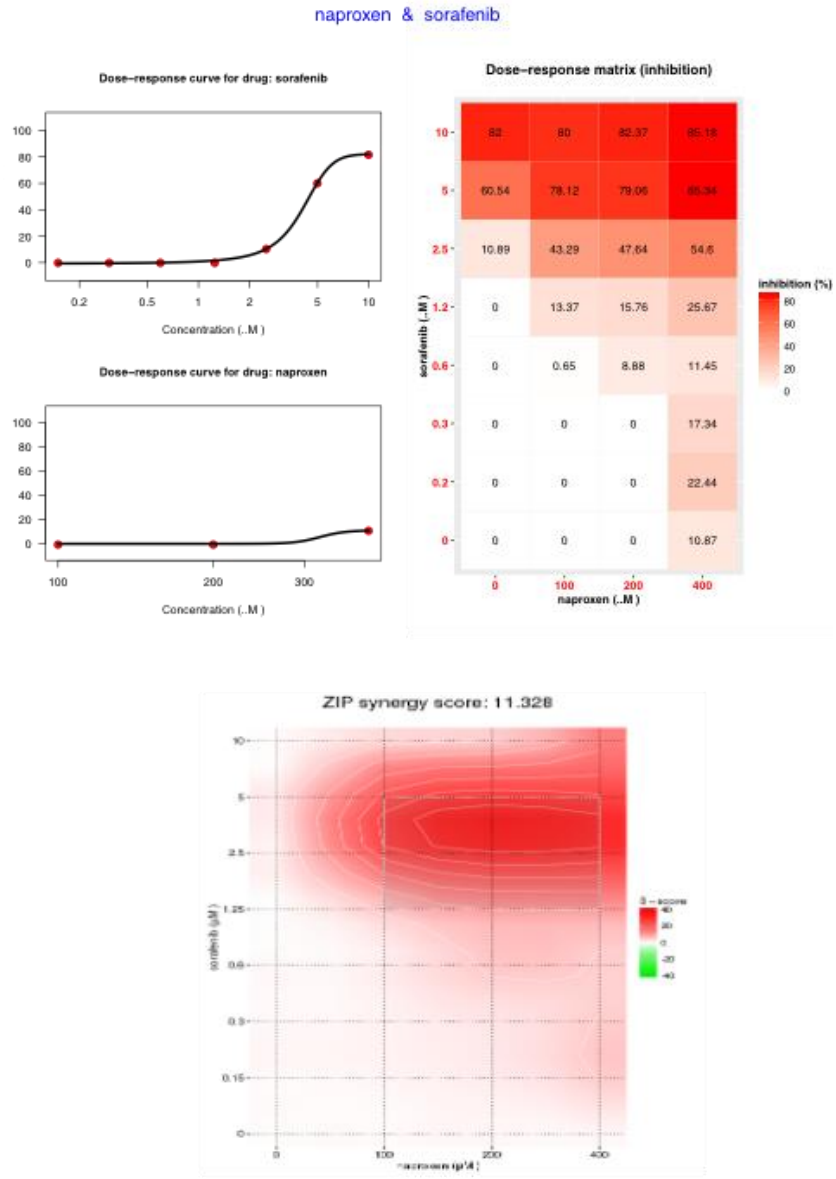

Figure A.2 Effect of combination on MCF12A -normal like cell line. MCF12A cell line was treated with the indicated dose of naproxen and sorafenib for 72h. Dose-response matrices were generated by NCI-SRB assay, and the Synergy score was calculated by Synergyfinder.

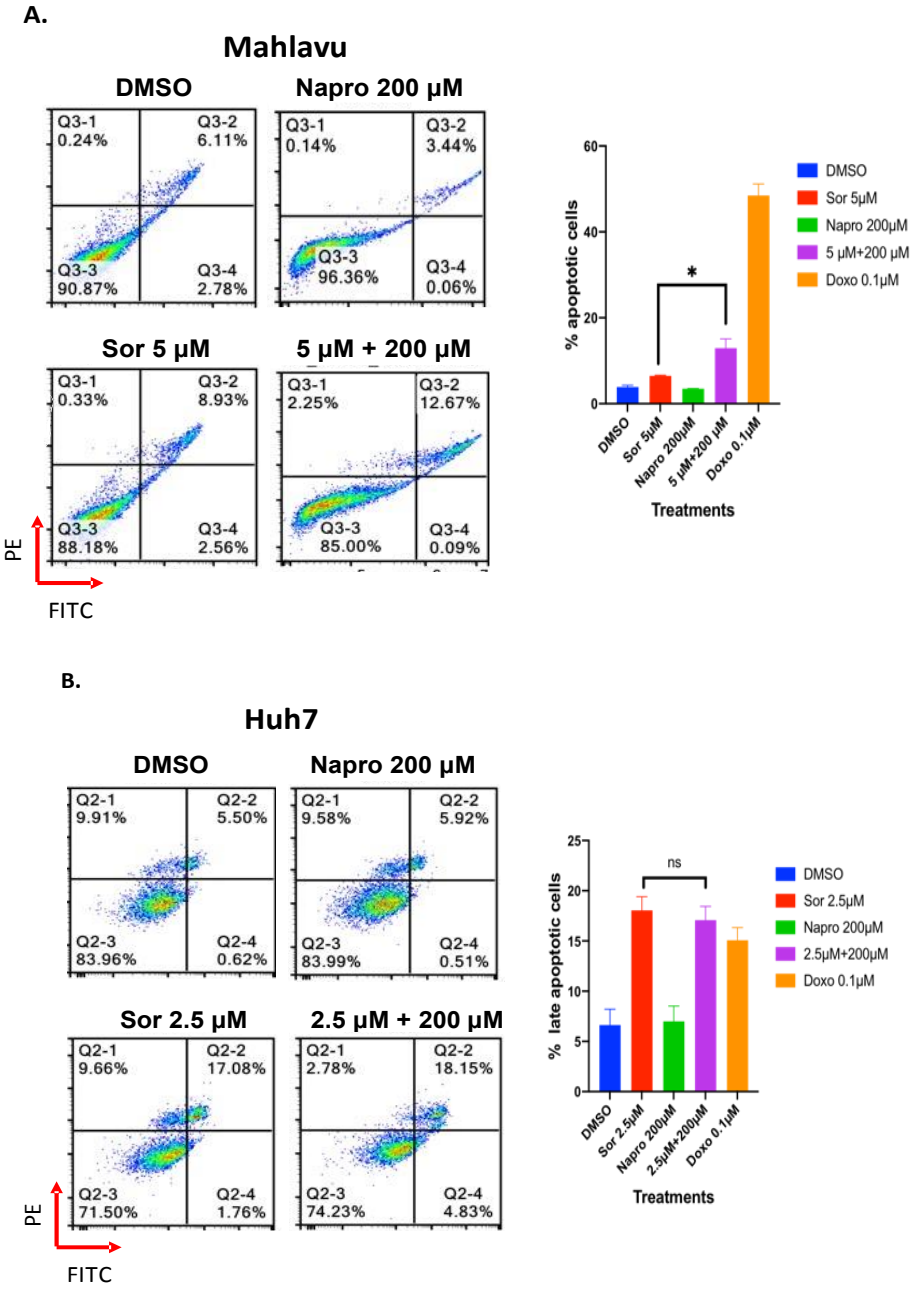

Figure A.3 Annexin-V assay of sorafenib and naproxen combination. 200 µM naproxen combined with the selected concentration of sorafenib 5 µM and 2.5 µM in Mahlavu **(A)** and Huh7 **(B)**, respectively. One-way ANOVA was applied for significance, and the bar graph represents percentages of late apoptosis cells in 72h.

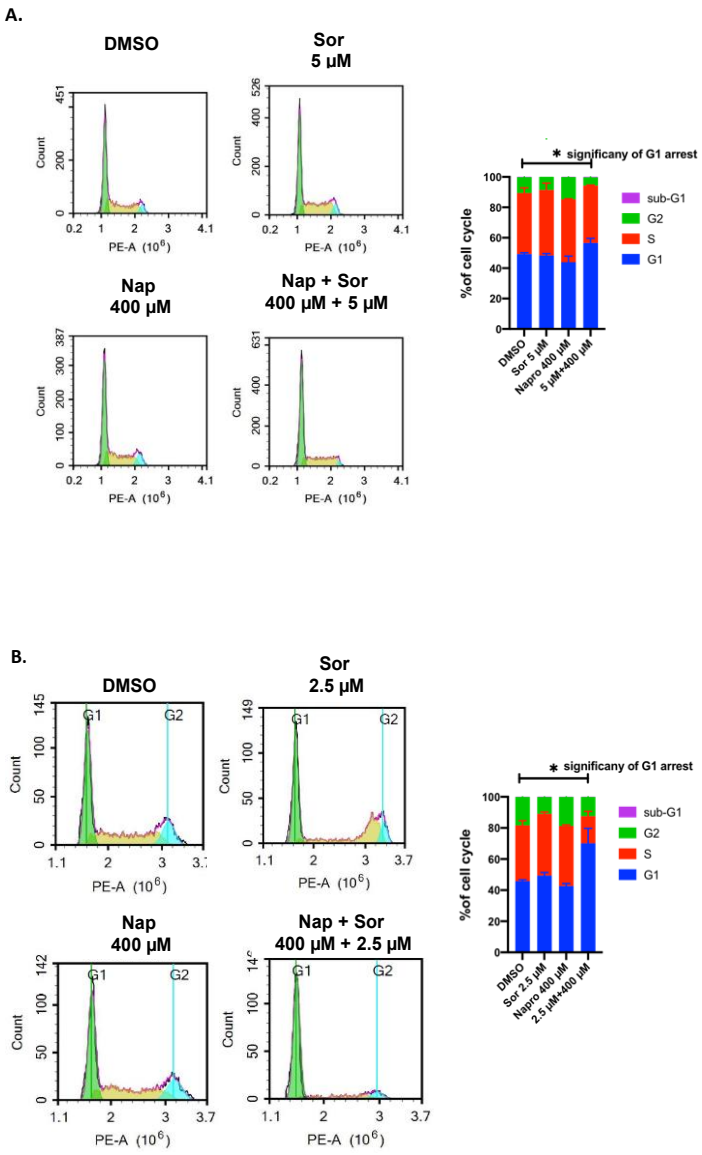

Figure A.4 Cell cycle analysis of sorafenib and naproxen combination in HCC cell lines. Mahlavu **(A)** and Huh7 **(B)** cells were treated with indicated concentrations of naproxen and sorafenib for 48h. One-way ANOVA was used to assess significance.